Int. J. Cancer: **119,** 484–492 (2006)

FAST TRACK

L-type amino acid transporter 1 as a potential molecular target in human astrocytic tumors

Hiroshi Nawashiro[1]*, Naoki Otani[1], Nariyoshi Shinomiya[2], Shinji Fukui[1], Hidetoshi Ooigawa[1], Katsuji Shima[1], Hirotaka Matsuo[3], Yoshikatsu Kanai[4] and Hitoshi Endou[4]

[1]*Department of Neurosurgery, National Defense Medical College, Tokorozawa, Saitama, Japan*
[2]*Department of Microbiology, National Defense Medical College, Tokorozawa, Saitama, Japan*
[3]*1st Department of Physiology, National Defense Medical College, Tokorozawa, Saitama, Japan*
[4]*Department of Pharmacology and Toxicology, Kyorin University School of Medicine, Mitaka, Tokyo, Japan*

L-type amino acid transporter 1 (LAT1) is a Na^+-independent neutral amino acid transport agency and essential for the transport of large neutral amino acids. LAT1 has been identified as a light chain of the CD98 heterodimer from C6 glioma cells. LAT1 also corresponds to TA1, an oncofetal antigen that is expressed primarily in fetal tissues and cancer cells. We have investigated for the first time, the expression of the transporter in the human primary astrocytic tumor tissue from 60 patients. LAT1 is unique because it requires an additional single membrane spanning protein, the heavy chain of 4F2 cell surface antigen (4F2hc), for its functional expression. 4F2hc expression was also determined by immunohistochemistry. Kaplan-Meier analyses demonstrated that high LAT1 expression correlated with poor survival for the study group as a whole ($p < 0.0001$) and for those with glioblastoma multiforme in particular ($p = 0.0001$). Cox regression analyses demonstrated that LAT1 expression was one of significant predictors of outcome, independent of all other variables. On the basis of these findings, we also investigated the effect of the specific inhibitor to LAT1, 2-aminobicyclo-2 (2,2,1)-heptane-2-carboxylic acid (BCH), on the survival of C6 glioma cells *in vitro* and *in vivo* using a rat C6 glioma model. BCH inhibited the growth of C6 glioma cells *in vitro* and *in vivo* in a dose-dependent manner. Kaplan-Meier survival data of rats treated with BCH were significant. These findings suggest that LAT1 could be one of the molecular targets in glioma therapy.

Key words: glioma; L-type amino acid transporter (LAT1); BCH

Glioma, especially glioblastoma, is the most common intrinsic brain tumor and with the worst prognosis in human malignancy. The cause of death of glioma patients is not a distant metastasis but the failure of local control of the tumor. The invasive nature of glioma often prevents total surgical excision. Adjuvant therapy for the residual tumor is therefore essential, however, conventional chemotherapy, immunotherapy, and radiotherapy has been proved to be of limited value.[1] Gene therapy for malignant glioma has been expected to be useful; however, no definitive clinical usefulness has been proved. Recently, several candidates for the molecular target of malignant tumors are advocated. One of them is the angiogenic and vascular proliferating factor.[2] The highly proliferating malignant tumor cells may need much substrate such as sugars and amino acids. If a specific upregulation of amino acid transport system in malignant tumor cells do exist, it could be a molecular target for therapy.

L-type amino acid transporter 1 (LAT1) is a Na^+-independent neutral amino acid transport agency and essential for the transport of large neutral amino acids through the plasma membrane.[3,4] LAT1 exhibits high affinity for several nutritionally essential amino acids such as leucine, isoleucine, valine, phenylalanine, tryptophan and methionine. The molecular nature of LAT1 was not characterized until 1998, when using expression cloning, a cDNA encoding a transporter subserving the LAT1 from a C6 rat glioma cell cDNA library was isolated by Kanai *et al.*[3] Since LAT1 is highly regulated in nature and upregulated upon the isolation and cultivation of cells, it is essential to examine the *in vivo* expression of LAT1 in brain tumor tissues.[5,6] The specific antibody to human LAT1, which recognizes both rodent and human LAT1, was generated. Using this antibody, we have investigated for the first time, the expression of the transporter in the human astrocytic tumor tissue. LAT1 is unique because it requires an additional single membrane spanning protein, the heavy chain of 4F2 cell surface antigen (4F2hc), for its functional expression.[3] When coexpressed with 4F2hc, LAT1 transports neutral amino acids with branched or aromatic side chains and does not accept basic amino acids or acidic amino acids.[3] 4F2hc expression was also determined by immunohistochemical staining with a polyclonal rabbit anti-human 4F2hc antibody. All astrocytic tumor cells clearly exhibited positive staining for LAT1 in variable degrees; however, we found strong expression of LAT1 in high-grade astrocytomas. On the basis of these findings, we also investigated the effect of the specific inhibitor to LAT1, 2-aminobicyclo-2(2,2.1)-heptane-2-carboxylic acid (BCH), on the growth of C6 glioma cells *in vitro* and *in vivo* using a rat C6 glioma model.[7]

Material and methods

Patients and tissues

All patients had primary astrocytic tumors of the brain. Patients were treated surgically for the first time between 1990 and 1999 in our hospital. Clinical data were obtained by retrospective chart review. Survival was determined from the date of initial surgery. Follow-up was available for all patients. Informed consent was obtained in all cases. Median follow-up time from resection of initial disease was 40.9 months.

Tumor specimens were obtained by surgical resection in all cases. Formalin-fixed, paraffin-embedded sections were stained with hematoxylin and eosin, and a histological and cytological diagnosis was made.

Histological diagnosis and tumor grading were performed according to the grading system established by WHO.[8] Fifteen specimens were diagnosed as Grade 2, 17 as Grade 3 and 28 as Grade 4 (glioblastoma multiforme (GBM)).

Immunohistochemistry for human LAT1 and 4F2hc in the glioma

LAT1 expression was determined by immunohistochemical staining with an affinity-purified polyclonal rabbit anti-human LAT1 antibody. Oligopeptides corresponding to amino acid residues 497–507 of human LAT1 (CQKLMQVVPQET) and amino acid residues 516–529 of human heavy chain of 4F2 cell surface antigen (4F2hc) (EPHEGLLLRFPYAAC) were synthesized. The N-terminal cystein residues were introduced for conjugation with

***Correspondence to:** Department of Neurosurgery, National Defense Medical College, 3-2 Namiki, Tokorozawa, Saitama 359-8513, Japan.
Fax: +81-4-2996-5207. E-mail: nawa1957@ndmc.ac.jp
Received 2 October 2005; Accepted 12 January 2006
DOI 10.1002/ijc.21866
Published online 22 February 2006 in Wiley InterScience (www.interscience.wiley.com).

Publication of the International Union Against Cancer

keyhole limpet hemocyamine. Antipeptide antibodies were produced as described elsewhere.[9] For immunohistochemical analysis, antisera were affinity-purified as described previously.[9]

Immunohistochemical staining was performed on paraffin sections using an avidin–biotinyl peroxidase complex method. Briefly, deparaffinized, rehydrated sections were treated with 0.6% hydrogen peroxide in methanol for 30 min to block endogenous peroxidase activity. After rinsing in 0.05 M tris-buffered saline containing 0.1% tween-20, the sections were incubated with anti-LAT1antiserum (1:250) or anti-4F2hc antiserum (1:500) overnight at 4°C. Thereafter, they were incubated with Envision (+) rabbit peroxidase (DAKO, Carpinteria, CA) for 30 min. The peroxidase reaction was performed using 0.02% 3,3′-diaminobenzidine tetrahydrochloride and 0.01% hydrogen peroxide in 0.05 M tris-HCl buffer, pH 7.4. Finally, nuclear counterstaining was performed with Mayer's hematoxylin. To verify the specificity of immunoreactions by absorption experiments, the tissue sections were treated with primary antibodies in the presence of antigen peptides (200 μg/ml).

Analysis of LAT1 and 4F2hc staining

Immunoreactivity was graded from – to +++ according to the percent of positive cells and the intensity of staining. The percentage of cells expressing LAT1 and 4F2hc was estimated by dividing the number of positively stained astrocytic tumor cells by the total number of tumor cells per high-power field. The cases in which all cells or more than 75% of the cells stained positively were considered diffuse staining: those in which less than 75% of the cells stained were considered patchy staining. More than 1,000 tumor cells were counted to determine the percentage of positive cells. The intensity of staining was determined and recorded as negative, weak, or strong. The cases in which weak patchy or not stained were considered (−); diffuse weak staining were considered (+); strong patchy staining were considered (++); and those strong diffuse staining were considered (+++). According to this grading protocol, 2 observers (HN and NO) of the authors, without prior knowledge of the clinical data, independently graded the staining intensity in all cases. To test the intraobserver variability, all sections were reassessed by one author (HN) after all first measurements had been completed. The time between the first and second assessments was at least 4 weeks. The interobserver variability was determined by comparing the values of the first measurements of 2 authors (HN and NO).

Proliferation rates determined by proliferating cell nuclear antigen immunostaining

The same tumor specimens were analyzed by immnohistochemistry with an anti-proliferating cell nuclear antigen (PCNA) monoclonal antibody (Novocastra Laboratories Ltd., Newcastle upon Tyne, UK). Paraffin-embedded tissue sections (3-μm thick) were employed for immunohistochemistry. After deparaffinization in xylene and blocking of endogenous peroxidase activity with 0.3% hydrogen peroxide in absolute methanol for 30 min at room temperature, the sections were incubated for 1 hr with anti-PCNA monoclonal antibody. The sections were washed with PBS, and treated with biotynyl anti-rabbit immunoglobulin for 10 min, then washed with PBS again and treated with peroxydase-labeled streptavidin for 5 min, and incubated in 3,3′-diaminobenzidine (DAB) solution, and then counterstained with methylgreen. Control study: (*i*) normal brain slices (negative control) (*ii*) adenocarcinoma (positive control) (*iii*) normal rabbit serum was used instead of the specific antibodies. The percentages of PCNA-positive cells were determined by counting 1,000–1,500 cells in at least 2 microphotographs of each section.

Statistical analysis

Survival was analyzed using the Kaplan-Meier method, and prognostic factors were assessed by log-rank analysis. Univariate and multivariate analyses were made of disease-specific survival (based on the number of patients who did not die from glioma). LAT1 and 4F2hc staining score, and other putative prognostic factors (age, gender, tumor histology, PCNA staining index) were used to stratify patients. A stepwise multivariate Cox regression analysis was also performed to further test the independence of LAT1 expression from other parameters. The distribution of the LAT1 score in relation to tumor and patient characteristics was investigated using the χ^2-test. Correlations between variables were obtained using Spearman's rank correlation. All tests were two-sided, and $p < 0.05$ was considered significant.

Cell line and culture condition

C6 rat glioma cell line was purchased from Dainippon Pharmaceutical Company (Osaka, Japan). Cells were maintained in a CO_2 incubator at 37°C by *in vitro* passage at 3–4-day intervals in Ham's F10 medium with 2 mM L-glutamine (GIBCO BRL, Grand Island, NY) supplemented with 15% horse serum (GIBCO BRL) and 2.5% fetal bovine serum (HyClone®). After the cells reached subconfluence, single-cell suspension was obtained by trypsinization and the numbers of cells were counted with a particle counter (Model PC-607, Erma, Tokyo, Japan). Then cell suspensions of desired concentrations were prepared and used for the following experiments.

Evaluation of cell survival in vitro *(colorimetric MTT assay)*

Reagents required for the colorimetric MTT (3-(4,5-dimethylthiazol-2-yl)-2,5-diphenyl tetrasolium bromide) assay were purchased from Chemicon International (Temecula, CA). Cells at a desired concentration were plated in 96-well flat-bottomed tissue culture trays (Falcon) and placed gently until they completely adhered to the bottom. Then the culture medium was replaced by a new one containing a desired concentration of BCH, and its effect on the cell growth was evaluated. The vehicle was culture medium used to introduce the BCH in cell cultures. At the end of the assay, 10 μl of MTT solution was added to each well and cells were incubated at 37°C for 4 hr. Then 100 μl of isopropanol/HCl solution was added to each well to dissolve the MTT formazan. Within an hour, the absorbance at a test wavelength of 595 nm and a reference wavelength of 655 nm ($OD_{595-655}$) was measured on an ELISA plate reader (Bio-Rad, Model 3550 microplate reader).

A rat glioma model

Adult male Wistar rats weighing 200 g were used for this study. Animals were maintained and experiments conducted according to guidelines established by the Institutional Animal Care and Use Committee of National Defense Medical College.

The rats were anesthetized with isoflurane in 30% oxygen and 70% nitrous oxide gas mixture through a facemask. The rats were fixed in a stereotactic head holder in a flat-skull position. A burr hole was made using a 1.4-mm diamond-tipped burr at the following coordinates: 1.5 mm anterior to bregma and 3.0 mm lateral of midline. A needle was inserted into the right caudate nucleus, depth 5.0 mm from the top of skull. C6 cells were prepared fresh from culture to ensure optimal viability of cells during tumor inoculation. Each rat was injected with 1.0×10^6 C6 cells in 10 μl phosphate-buffered saline-glucose medium. After injection, injector remained for 5 min to allow the injected cell suspension to come to equilibrium inside the brain.

For continuous infusion of the tumor inoculation site, each rat was implanted with an osmotic minipump-brain infusion assembly 1 day or 8 days after tumor inoculation. The minipump (average infusion rate, 5.0 l/hr; Alzet model 2ML2; Alza, Palo Alto, CA) was filled with either vehicle alone (saline, control), 50 mM D-mannitol, or a desired concentration (50 mM or 230 mM) of BCH. The brain infusion assembly consisted of a catheter tubing and a stainless steel cannula with two-depth adjustment spacers to obtain stereotaxically correct depth. The tubing-cannula assembly was also filled with the appropriate solution and joined to the pump.

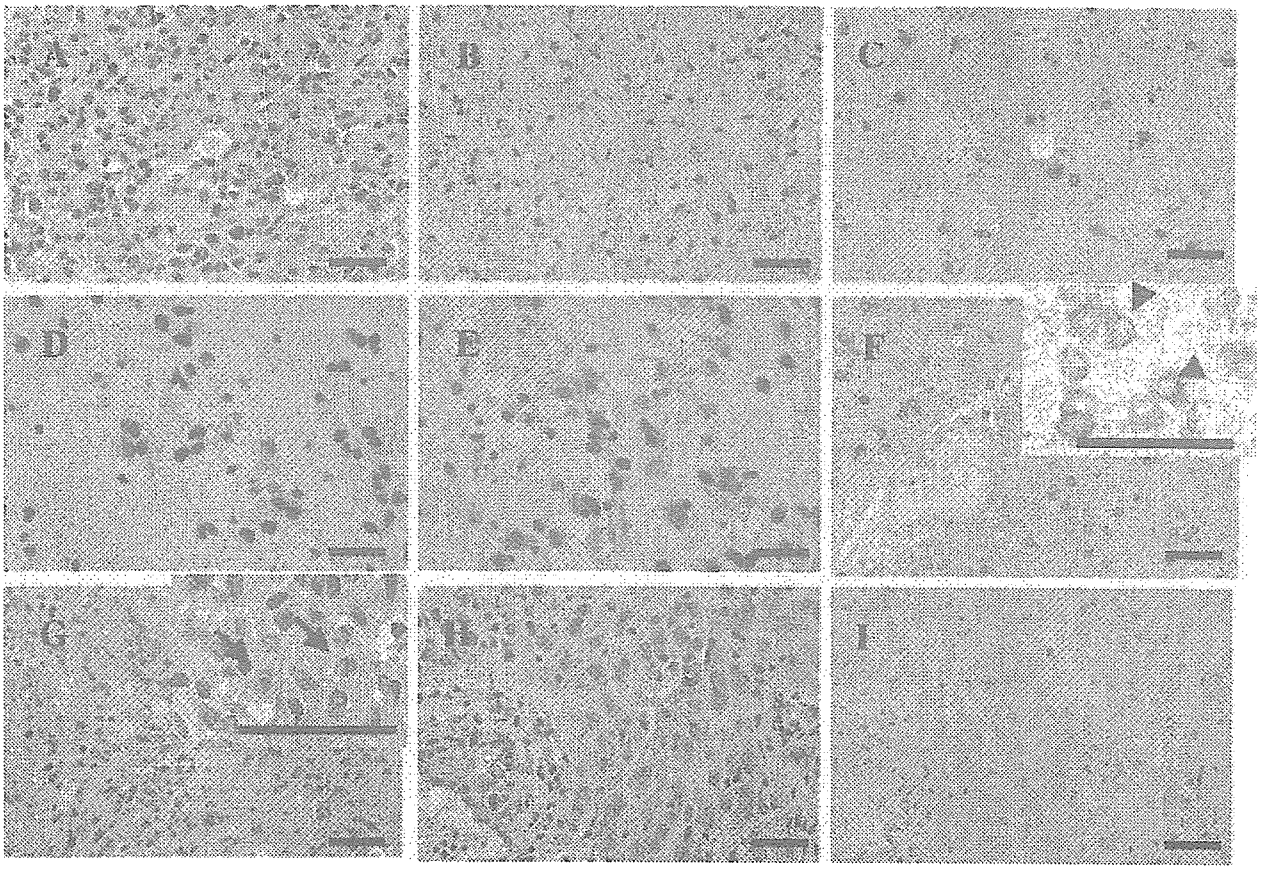

FIGURE 1 – (*a*) Glioblastoma with diffuse weak (+) immunoreactivity for LAT1. (*b*) Low grade glioma with diffuse weak (+) immunoreactivity for LAT1. (*c*) Anaplastic astrocytoma with strong patchy (++) staining for LAT1. (*d*) Anaplastic astrocytoma with strong patchy (++) staining for 4F2hc. (*e*) Anaplastic astrocytoma (the same specimen as shown in *d*) with diffuse strong (+++) staining for LAT1. (*f*) Anaplastic astrocytoma with intense immunoreactivity for LAT1 observed predominantly on the plasma membrane (arrow heads). Inset at higher magnification. (*g*) Glioblastoma with strong diffuse (+++) cytoplasmic staining (arrows) for LAT1. Inset at higher magnification. (*h*) Glioblastoma with strong diffuse (+++) cytoplasmic staining for LAT1. (*i*) In the absorption experiments, the LAT1 immunostainings were diminished, confirming the specificity of the immunoreaction (the same specimen as shown in H). Immunoreactions were visualized with diaminobenzidine and nuclear counterstaining was performed with Mayer's hematoxylin. All bars = 20 μm.

One day or 8 days after tumor inoculation, the cannula was inserted at the inoculation site and secured in position with dental cement. The osmotic pump was housed in a subcutaneous pocket in the midscapular area of the back of the rat for 28 days. Animals recovered from anesthesia and resumed their previous activity in cages. The animals were housed individually to prevent dislodging of the brain infusion assembly.

Fifty-one rats were divided into 6 experimental groups. Group 1 ($n = 9$) were given 230 mM of BCH 1 day after tumor inoculation. Group 2 ($n = 9$) were given the saline 1 day after tumor inoculation. In Group 3 ($n = 7$), animals were given 230 mM of BCH 8 days after tumor inoculation. Group 4 ($n = 12$) received 50 mM of BCH 8 days after tumor inoculation. This dose was selected because cell survival was disturbed *in vitro* when BCH was added at a concentration of more than 25 mM. Group 5 ($n = 7$) were given the saline 8 days after tumor inoculation. Group 6 ($n = 7$) were given 50 mM D-mannitol 8 days after tumor inoculation.

After tumor inoculation, the body weight of rats was measured and recorded every day. All survivors were sacrificed 22 days after implantation. They were deeply anesthetized with intraperitoneal pentobarbital (100 mg/kg). Animals were perfused transcardially with normal saline followed by 4% buffered paraformaldehyde. The brains were removed and embedded in paraffin after fixation in 4% buffered paraformaldehyde followed by 0.1 mmol/l PBS (pH 7.4) for 24 hr at 4°C. Serial coronal sections (5-μm-thick) were prepared. The serial sections were mounted onto silanated slides and were used for histology and histochemistry. The sections were stained with hematoxylin and eosin to confirm the tumor. The same tumor specimens were analyzed by immunohistochemistry with an anti-PCNA monoclonal antibody as described above. The extent of the tumor at 20 predetermined levels was measured with the computer-assisted image analyzing system (NIH image 1.57). The tumor volume was calculated by taking the sum of the tumor areas of the different brain slices times the thickness of the slices. Tumor volumes and the percentages of PCNA-positive cells in each animals were analyzed by analysis of variance (ANOVA) followed by the Bonferroni/Dunn test to ascertain significance between groups. The body weight of each animal was analyzed by repeated-measures ANOVA. Statistical significance was set at $p < 0.05$.

Results

Sixty specimens were obtained from 60 patients with primary astrocytic gliomas. Twenty-nine patients were male and 31 were female. They ranged from 11 to 88 yr in age (mean, 45.1 years ± 19.3). All patients had Karnofsky performance scores of at least 70 at diagnosis. Patients were treated with surgery and adjuvant chemoradiation therapy (consisting of ACNU, interferon β, local

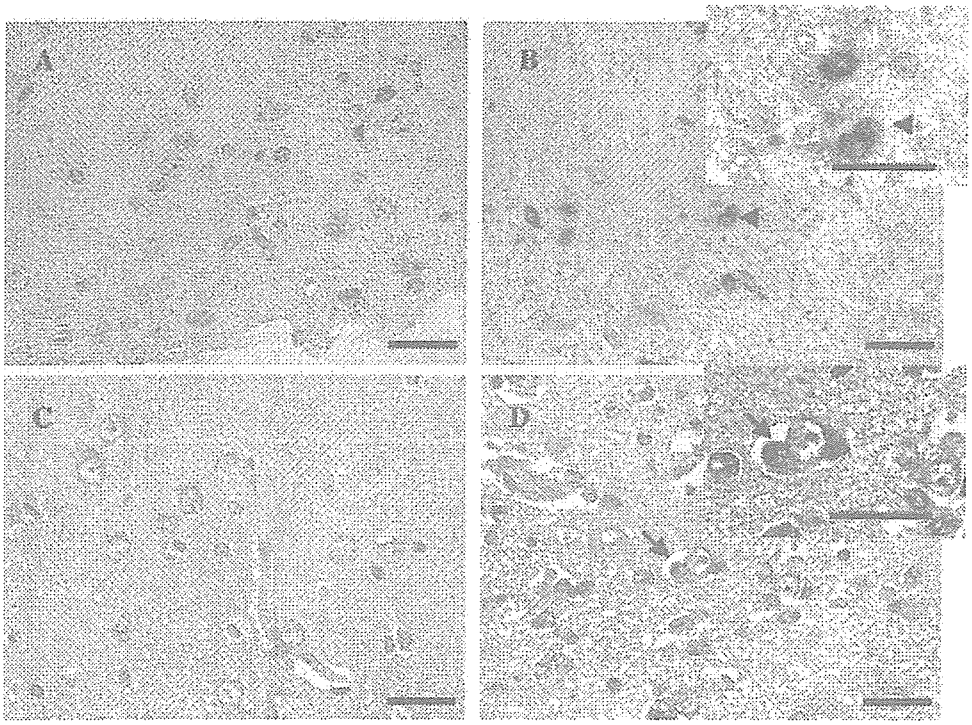

FIGURE 2 – (*a*) Control LAT1 staining on normal uninvolved brain. (*b*) Glioblastoma cells of the same patient in the border zone with strong staining for LAT1 showing perineuronal satellitosis (arrow heads). (*c*) Control 4F2hc staining on normal uninvolved brain in the same patient. (*d*) Glioblastoma cells of the same patient in the border zone with weak staining for 4F2hc showing perineuronal satellitosis (arrows). All bars = 20 μm.

TABLE I – CORRELATION OF LAT1 AND 4F2hc STAINING WITH CLINICAL AND HISTOPATHOLOGICAL FEATURES OF ASTROCYTIC TUMORS

	LAT1			*p*	4F2hc			*p*
	(+) (*n* = 21)	(++) (*n* = 18)	(+++) (*n* = 21)		(+) (*n* = 27)	(++) (*n* = 22)	(+++) (*n* = 11)	
Age (yr)								
0–19	6	2	0	0.0658	4	4	0	0.731
20–39	5	4	3		6	4	2	
40–59	7	8	8		11	8	4	
60+	3	4	10		6	6	5	
Tumor histology								
Low-grade astrocytoma	10	4	1	0.0059	8	7	0	0.1074
AA	4	8	5		10	4	3	
GBM	7	6	15		9	11	8	
Gender								
Male	9	6	14	0.0953	15	7	7	0.1354
Female	12	12	7		12	15	4	
PCNA index (%)								
<5	7	4	0	0.0075	6	5	0	0.0264
5–30	10	10	8		16	9	3	
>30	4	4	13		5	8	8	
4F2hc								
(+)	12	9	6	0.0098				
(++)	8	8	6					
(+++)	1	1	9					

external beam radiation) for all patients with GBM or anaplastic astrocytoma and adjuvant radiation therapy for most patients with low-grade astrocytoma. There were 28 GBMs, 17 anaplastic astrocytomas and 15 low-grade fibrillary astrocytomas.

Qualitative immunohistochemical analysis for LAT1 and 4F2hc

LAT1 and 4F2hc immunoreactivity was observed in all the tumor specimens examined. LAT1 immunostaining was observed predominantly on the plasma membrane and astrocytic process (Figs. 1*c* and 1*f*). In cases of strong diffuse LAT1 staining in tumor cells, intense cytoplasmic staining was also evident (Figs. 1*g* and 1*h*). In sections containing areas of normal cortex adjacent to the tumor, infiltrating tumor cells showed more intense LAT1 staining (Fig. 2*b*). Examples of LAT1 and 4F2hc immunostaining of the same specimen are shown in Figures 1*d* and 1*e*. In the absorption experiments in which tissue sections were treated with primary antibodies in the presence of antigen peptides, the immunostaining was drastically decreased, confirming the specificity of the immunoreaction (Fig. 1*i*). The nuclear staining for LAT1 might be artifactual; however, the nuclear and perinuclear staining

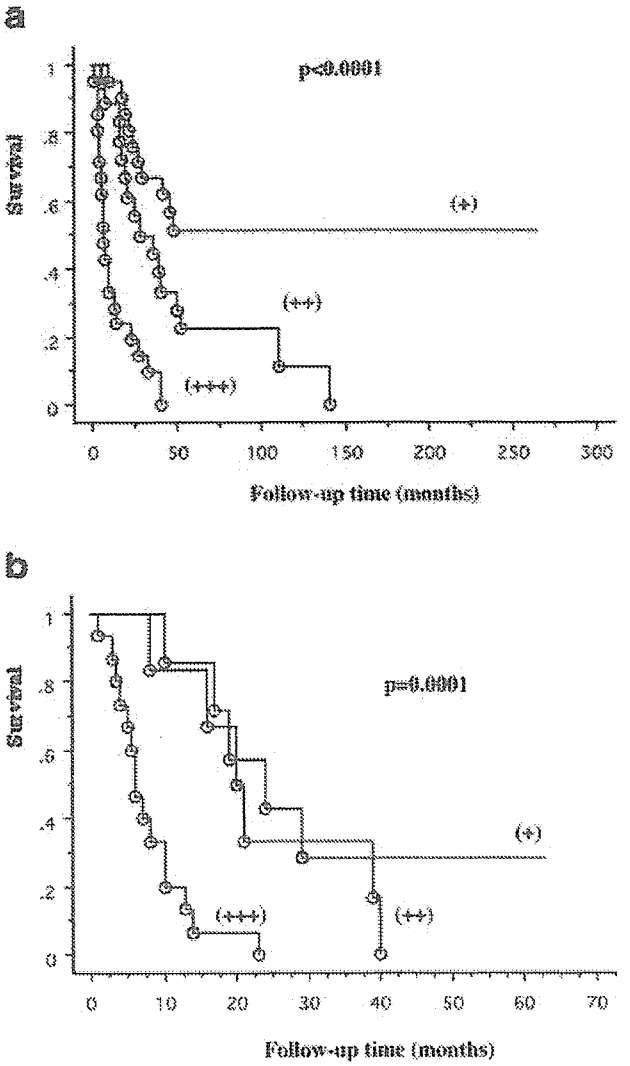

FIGURE 3 – (*a*) Actuarial survival (Kaplan-Meier method) of patients with astrocytoma whose tumors had LAT1 immunostaining of (+), (++) or (+++). (*b*) Actuarial survival (Kaplan-Meier method) of patients with GBM whose tumors had LAT1 immunostaining of (+), (++) or (+++).

was also decreased in the absorption experiments. LAT1 and 4F2hc immunostaining on normal uninvolved brain are shown in Figures 2*a* and 2*c*. No significant immunostaining in neurons or astrocytes was seen in the uninvolved normal brain. The intraobserver reproducibility of scoring was high (correlation coefficient, 0.93; $p < 0.0001$; coefficient of variance, 29.7%). The interobserver reproducibility of scoring was also high (correlation coefficient, 0.9; $p < 0.001$; coefficient of variance, 31.1%).

Correlation of LAT1 and 4F2hc staining with clinical and histopathological features

LAT1 immunostaining did not correlate with patient age or gender (Table I). However, the intensity of LAT1 staining was greater in GBMs than in low-grade astrocytomas (Table I). The grade of LAT1 staining increased with glioma grade, and this finding was statistically significant. The grade of LAT1 staining correlated statistically with PCNA index ($p = 0.0075$) and with 4F2hc staining ($p = 0.0098$) (Table I). The grade of 4F2hc staining also correlated statistically with PCNA index ($p = 0.0264$).

TABLE II – UNIVARIATE ANALYSIS OF PROGNOSTIC FACTORS FOR SURVIVAL

	No. of patients	3-yr survival (%)	*p* (log rank)
Age (yr)			
0–19	8	75.0	0.0006
20–39	12	41.7	
40–59	23	43.5	
60+	17	5.9	
Tumor histology			
Low-grade astrocytoma	15	80.0	<0.0001
AA	17	35.3	
GBM	28	10.7	
Gender			
Male	29	20.7	0.0227
Female	31	54.8	
PCNA index (%)			
<5	11	63.6	0.0392
5–30	28	39.3	
>30	21	19.0	
LAT1			
(+)	21	61.9	<0.0001
(++)	18	44.4	
(+++)	21	0.0	
4F2hc			
(+)	27	40.7	0.0183
(++)	22	45.5	
(+++)	11	9.1	

Correlation with patient survival

Kaplan-Meier survival plots for all patients showed a statistically significant association between high grade of LAT1 staining and poor outcome ($p < 0.0001$; Fig. 3*a*, Table II). Because survival of patients with glioma has been associated with several clinicopathological variables, we attempted to define the relative contribution of LAT1 immunostaining to survival by using multivariate Cox regression analyses with 6 variables (age, tumor histology, gender, PCNA index, LAT1 staining and 4F2hc staining). In the initial univariate analysis, age ($p = 0.0006$), tumor histology ($p < 0.0001$), 4F2hc staining ($p = 0.0183$), gender ($p = 0.0227$), PCNA index ($p = 0.0392$), and LAT1 staining ($p < 0.0001$) were all significant (Table II). For the multivariate analysis, we used the backward stepwise (Wald) method, in which variables were removed at each step, based on a 0.05 level of significance. At the final step, the last 3 variables, tumor histology ($p < 0.0001$), LAT1 staining ($p = 0.0004$), and age of patients ($p = 0.0244$) were found to be significant and independent of one another (Table III).

To evaluate the effect of high LAT1 staining grade within tumor grades, we analyzed the GBM subgroup for an association between LAT1 staining and survival. We found that GBM patients with tumors of high LAT1 staining grade had a statistically significant poorer prognosis than did those with tumors of low LAT1 staining grade ($p = 0.0001$ log-rank) (Fig. 3*b*). We also found that patients with low grade atrocytomas of high LAT1 staining had a statistically poor prognosis ($p = 0.0035$ log-rank). In the anaplastic astrocytoma group, no difference in survival was found, but the numbers of patients in this group was too small for accurate statistical sampling.

In vitro *effect of BCH on the survival of C6 glioma cells*

First, to ascertain the linearity of the MTT assay in C6 glioma cells, we performed serial dilution of the cells, and effect of cell number on the colorimeter reading was observed. The $OD_{595-655}$ well correlated with the actual number of the viable cells in the tested range. Accordingly, the cell number to give $OD_{595-655}$ value of 0.5 (namely 25,000 cells/well) was used for the following experiment.

Effect of the various concentration of BCH (from 1 to 100 mM) on the survival of C6 glioma cells was serially observed by MTT assay (Fig. 4). In the control (without BCH), cells continuously

TABLE III – MULTIVARIATE COX REGRESSION ANALYSIS OF THE FACTORS ASSOCIATED WITH SURVIVAL

Step	Variable	Relative risk (95% CI)	p (log-rank)
The first	Age (yr)		0.0499
	0–19	1.040 (0.226–4.790)	0.9600
	20–39		
	40–59[1]	1.049 (0.404–2.719)	0.9220
	60+	3.073 (1.173–8.048)	0.0223
	Tumor histology		<0.0001
	Low-grade astrocytoma[1]		
	AA	3.673 (0.636–21.207)	0.0208
	GBM	13.894 (4.287–45.028)	<0.0001
	LAT1		0.0059
	(+)	0.179 (0.062–0.516)	0.0014
	(++)	0.405 (0.167–0.982)	0.0455
	(+++)[1]		
	4F2hc		0.4627
	(+)	1.455 (0.614–3.451)	0.3945
	(++)	0.925 (0.358–2.391)	0.8714
	(+++)[1]		
	Gender		
	Male	1.578 (0.764–3.260)	0.2180
	Female[1]		
	PCNA (%)		0.7026
	<5	0.376 (0.248–2.186)	0.5813
	5–30	0.755 (0.384–1.483)	0.4139
	>30[1]		
The final	Age (yr)		0.0244
	0–19	0.824 (0.192–3.538)	0.7948
	20–39[1]		
	40–59	0.951 (0.377–2.402)	0.9159
	60+	2.990 (1.162–7.697)	0.0231
	Tumor histology		<0.0001
	Low-grade astrocytoma[1]		
	AA	4.153 (1.305–13.218)	0.0159
	GBM	11.310 (3.819–33.495)	<0.0001
	LAT1		0.0004
	(+)	0.167 (0.065–0.430)	0.0002
	(++)	0.303 (0.139–0.660)	0.0026
	(+++)[1]		

CI, confidence interval.
[1]Reference category.–[2]Potential prognostic factors selected from Table II were used.

increased in number and the $OD_{595-655}$ value at day 5 showed more than 1.0. In contrast, almost complete suppression of the cell growth was observed when 25 mM BCH was added to the culture medium. When BCH was added at a concentration of more than 25 mM, cell survival was disturbed and a decrease in the $OD_{595-655}$ value was observed. BCH at a concentration of 1–10 mM revealed a limited effect. We confirmed that this growth inhibitory effect of the BCH on C6 glioma cells was not due to high osmolarity of the BCH-added culture medium since addition of the equivalent molarity of D-mannitol showed no remarkable effect on the growth of C6 glioma cells (data not shown).

Effects of BCH on tumor sizes in vivo *and on survival of rats after tumor inoculation*

The volume of tumor averaged 77.9 ± 16.7 mm^3 in Group 1 (n = 9) (BCH230/1 day), 146.8 ± 21.4 mm^3 in Group 2 (n = 9) (saline/1 day), 95.3 ± 13.6 mm^3 in Group 3 (n = 7) (BCH230/8 days), 109.9 ± 12.1 mm^3 in Group 4 (n = 12) (BCH50/8 days), 144.7 ± 19.1 mm^3 in Group 5 (n = 7) (saline/8 days), and 130.1 ± 21.8 mm^3 in Group 6 (n = 7) (mannitol50/8 days), respectively (mean ± SE) (Fig. 5). The volume of tumor in Group 1 was significantly smaller than that in Group 2 (p = 0.022). The volume of tumor in Group 3 was also smaller than that in Group 5, but the difference was not significant (p = 0.057). All animals lost weight within 6–17 days after tumor inoculation and continuously lost it thereafter. The time point of maximal body weight was significantly prolonged in the animals treated with 230 mM of BCH (Group 1) when compared with that of Group 2 (p = 0.026). Kaplan-Meier survival data of rats in Group 1 were significant (Fig. 6), compared to that of rats in Group 2 (p = 0.016 log-rank). BCH, saline or D-mannitol administration to a concentration of 50–230 mM was not associated with occurrence of seizures, or changes in behavior (such as sluggishness or inability to eat) in rats without tumor cells. The percentage of PCNA-positive cells in Group 1 was significantly smaller than that in Group 2 (p = 0.0182).

Discussion

We have demonstrated for the first time that high LAT1 immunostaining predicts a poor prognosis in patients with astrocytic brain tumors in general and in patients with GBM or low grade astrocytoma in particular. However, LAT1 was the second strongest predictor of outcome in general. It is speculated that LAT1 expression is upregulated so as to provide cells with essential amino acids for high levels of protein synthesis associated with cell activation and also to support rapid growth or continuous proliferation. Indeed, we found that high LAT1 expression correlated with high proliferating potential of the tumor estimated by PCNA immunohistochemistry. LAT1 also corresponds to TA1, an oncofetal antigen that is expressed primarily in fetal tissues and cancer cells.[10] A high level of LAT1 expression was also detected in human tumor cell lines such as stomach signet ring cell carcinoma (KATOIII), malignant melanoma (G-361), and lung small-cell carcinoma (RERF-LC-MA) by Northern blot analysis.[3] The database search indicated that partial or incomplete sequences of LAT1 (E16, TA1 and ASUR4b) were already reported.[5,6,11] E16 and ASUR4b were identified to be up-regulated upon the mitogenic stimulation of lymphocytes and the stimulation of A6 epithelial cell line by aldosterone, respectively,[5,11] suggesting highly regulated nature of LAT1 gene expression. TA1 was identified as

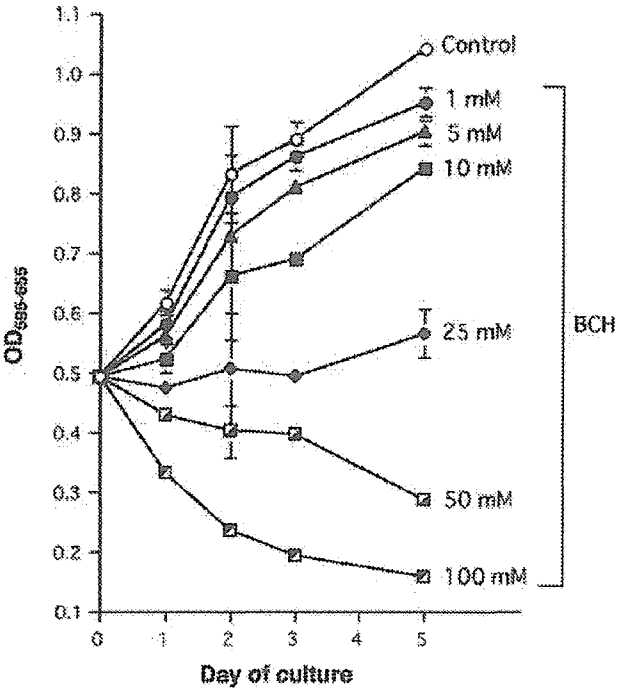

FIGURE 4 – Effect of the various concentration of BCH (from 1 to 100 mM) on the survival of C6 glioma cells was serially observed by MTT assay.

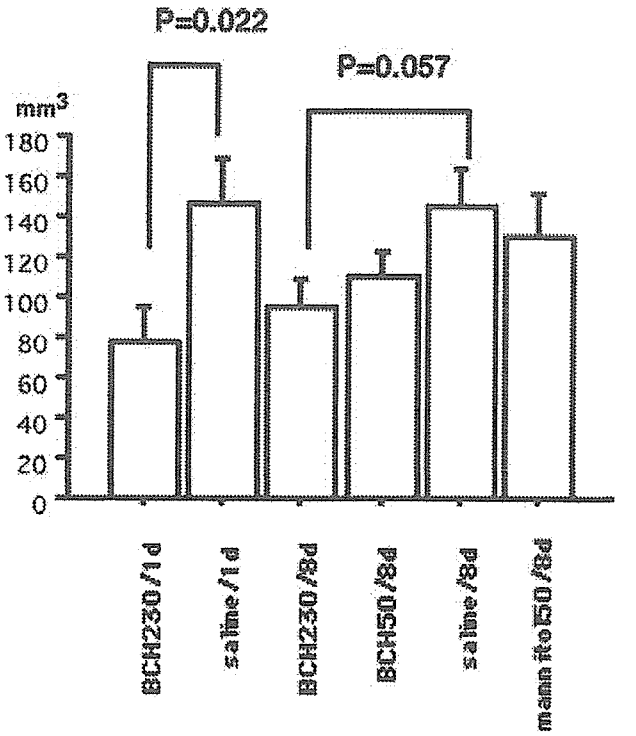

FIGURE 5 – Average tumor volumes ± SE in each group are shown. Fifty-one rats were divided into 6 experimental groups. Group 1 (BCH230/1 day) (n = 9) were given 230 mM of BCH 1 day after tumor inoculation. Group 2 (saline/1 day) (n = 9) were given the saline 1 day after tumor inoculation. In group 3 (BCH230/8 days) (n = 7), animals were given 230 mM of BCH 8 days after tumor inoculation. Group 4 (BCH50/8 days) (n = 12) received 50 mM of BCH 8 days after tumor inoculation. Group 5 (saline/8 days) (n = 7) were given the saline 8 days after tumor inoculation. Group 6 (mannitol50/8 days) (n = 7) were given 50 mM D-mannitol 8 days after tumor inoculation. Statistical significance was determined by ANOVA followed by Bonferroni/Dunn test.

a tumor-associated sequence with the oncofetal pattern of expression in rat liver.[6] TA1 immunoreactivity was abundant in human colon cancer *in vivo* but barely detected in surrounding normal colon tissue,[12] confirming the high level of expression of LAT1 protein in tumor cells. The 4F2hc is thought to be involved in the trafficking and regulation of system L neutral amino acid transport in mammalian cells as mentioned previously. Because 4F2hc is essential for LAT1 to be functional, the level of 4F2hc expression would greatly affect the formation of functional system L transporters in the plasma membrane. We found that high 4F2hc immunoreactivity also correlated with high LAT1 expression; however, LAT1 staining had a major impact on survival rate. Involvement of LAT1 in tumor progression is also strongly suggested by a recent study that showed that up-regulation of the CD98 complex, but not the CD98 heavy chain (4F2hc) alone, in Balb3T3 cells resulted in tumorigenicity in nude mice.[13] LAT1 has been shown to be a transiently expressed membrane protein with the rapid degradation signal AUUUA.[5] Nakamura *et al.* demonstrated that LAT1 is expressed minimally at the plasma membrane in cancer cells, remaining mostly in the Golgi area, and requires 4F2hc to be sorted to the cell surface.[14] The immunoreactivity of LAT1 in the plasma membrane may represent its function. We did not differentiate the immunoreactivity of both cytosol and plasma membrane when estimating the grade of immunoreactivity of LAT1. However, the overall immunoreactivity for LAT1 did correlate well with the prognosis of patients with astrocytic tumors. Cytoplasmic LAT1 immunoreactivity may represent an intracellular pool of LAT1, and may correlate with the biological activity of cells.

To clarify the role of LAT1 in glioma cells, we tested a relatively specific inhibitor to LAT1, BCH, and found that BCH suppressed strongly C6 glioma cell growth *in vitro*. In addition, BCH also inhibited mortality of rats treated with C6 glioma cells. BCH at a concentration of 25 mM showed no significant effect on normal human astrocytes *in vitro* (data not shown). BCH is a nonmetabolizable artificial amino acid and a transportable inhibitor for LAT1. Yanagida *et al.* showed that a high-affinity substrate, leucine, and a low-affinity substrate, glutamine, but not a nonsubstrate, alanine, were effluxed *via* LAT1 by the application of leucine in the medium, confirming that LAT1 is an amino acid exchanger.[15] This, furthermore, suggests that the substrate selectivity of the intracellular substrate binding site of LAT1 is similar to that of the extracellular substrate binding site. Amino acids are released *via* LAT1 in exchange for the influx of amino acids; thus, no net amino acid influx should be observed. Glutamine, which is abundantly present in cells and generated intracellularly, is transported by LAT1 albeit with low affinity, consistent with a previous report for *Xenopus* LAT1.[4] Yanagida *et al.* further demonstrated that intracellularly loaded glutamine is effluxed in exchange for extracellularly applied leucine.[15] Therefore, they propose that extracellular high-affinity LAT1 substrates, most of which are essential amino acids, are taken up by cells *via* LAT1 driven by the exchange for intracellular-glutamine, which results in the net influx of essential amino acids.[15] An interesting finding of the Northern blot analysis of the tumor cell line is that the expression level of 4F2hc is quite varied among tumor cell lines, particularly in leukemia cell lines.[15] Yanagida *et al.* found 3 leukemia cell lines in which 4F2hc messages were not detected.[15] In those cell lines that lack 4F2hc expression, LAT1 was still expressed, suggesting different mechanisms of regulation in LAT1 and 4F2hc gene expression. Consistent with this, it was shown that LAT1 and 4F2hc respond differently to amino acid availability in rat hepatic cells.[16]

Several clinical investigations demonstrated the significant relation of the uptake of radiolabeled amino acid in gliomas and proliferation, biological aggressiveness or histological grading of

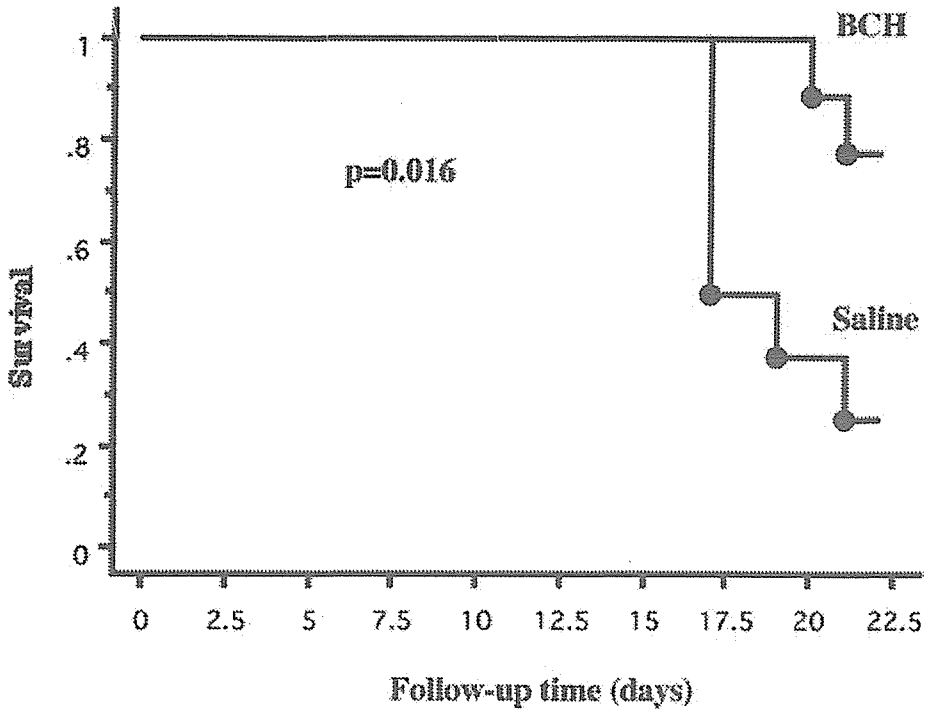

FIGURE 6 – Kaplan-Meier survival curves of C6 glioma-bearing rats after implantation of tumor cells.

these tumors.[17,18] A significant correlation of iodine-123–methyl-tyrosine (IMT) uptake in gliomas and the expression of the proliferation marker Ki-67 has been reported.[18] Recent studies also demonstrated significant longer survival times in patients with cerebral gliomas with low amino acid uptake than in gliomas with high amino acid uptake.[19] The results of this study support the hypothesis that the uptake of radiolabeled amino acids such as IMT is dependent on the proliferative activity of human gliomas. It is noteworthy that in cultured human glioma cells, membrane transport of IMT is dominated by BCH-sensitive transport system, LAT1.[20,21] LAT1-mediated IMT transport and 4F2 antigen expression are dependent on proliferation rate of human glioma cells *in vitro* and are significantly correlated to each other.[20] These data give further support to the involvement of the LAT1 in cell proliferation.[20,22] Thompson and coworkers recently reported the role of LAT1 as a potential therapeutic target in hepatic tumor cells *in vitro*.[23]

The present study suggests that LAT1 may play an important role in human high-grade gliomas. In addition, inhibitors to LAT1 may be an effective therapeutic option for high-grade gliomas.

References

1. Shrieve DC, Alexander E, III, Black PM, Wen PY, Fine HA, Kooy HM, Loeffler JS. Treatment of patients with primary glioblastoma multiforme with standard postoperative radiotherapy and radiosurgical boost: prognostic factors and long-term outcome. J Neurosurg 1999;90:72–7.
2. Millauer B, Shawver LK, Plate KH, Risau W, Ullrich A. Glioblastoma growth inhibited in vivo by a dominant-negative Flk-1 mutant. Nature 1994;367:576–9.
3. Kanai Y, Segawa H, Miyamoto K, Uchino H, Takeda E, Endou H. Expression cloning and characterization of a transporter for large neutral amino acids activated by the heavy chain of 4F2 antigen (CD98). J Biol Chem 1998;273:23629–32.
4. Mastroberardino L, Spindler B, Pfeiffer R, Skelly PJ, Loffing J, Shoemaker CB, Verrey F. Amino-acid transport by heterodimers of 4F2hc/CD98 and members of a permease family. Nature 1998;395:288–91.
5. Gaugitsch HW, Prieschl EE, Kalthoff F, Huber NE, Baumruker T. A novel transiently expressed, integral membrane protein linked to cell activation. Molecular cloning via the rapid degradation signal AUUUA. J Biol Chem 1992;267:11267–73.
6. Sang J, Lim YP, Panzica M, Finch P, Thompson NL. TA1, a highly conserved oncofetal complementary DNA from rat hepatoma, encodes an integral membrane protein associated with liver development, carcinogenesis, and cell activation. Cancer Res 1995;55:1152–9.
7. Bruce JN, Falavigna A, Johnson JP, Hall JS, Birch BD, Yoon JT, Wu EX, Fine RL, Parsa AT. Intracerebral clysis in a rat glioma model. Neurosurgery 2000;46:683–91.
8. Kleihues P, Cavenee WK. Pathology and genetics of tumours of the nervous system. Lyon, France: IARC, 2000. p 6.
9. Chairoungdua A, Segawa H, Kim JY, Miyamoto K, Haga H, Fukui Y, Mizoguchi K, Ito H, Takeda E, Endou H, Kanai Y. Identification of an amino acid transporter associated with the cystinuria-related type II membrane glycoprotein. J Biol Chem 1999;274:28845–8.
10. Mannion BA, Kolesnikova TV, Lin SH, Wang S, Thompson NL, Hemler ME. The light chain of CD98 is identified as E16/TA1 protein. J Biol Chem 1998;273:33127–9.
11. Spindler B, Mastroberardino L, Custer M, Verrey F. Characterization of early aldosterone-induced RNAs identified in A6 kidney epithelia. Pflugers Arch 1997;434:323–31.
12. Wolf DA, Wang S, Panzia MA, Bassily NH, Thompson NL. Expression of a highly conserved oncofetal gene, TA1/E16, in human colon carcinoma and other primary cancers: homology to *Schistosoma mansoni* amino acid permease and *Caenorhabditis elegans* gene products. Cancer Res 1996;56:5012–22.
13. Shishido T, Uno S, Kamohara M, Tsuneoka-Suzuki T, Hashimoto Y, Enomoto T, Masuko T. Transformation of BALB3T3 cells caused by over-expression of rat CD98 heavy chain (HC) requires its association with light chain: mis-sense mutation in a cysteine residue of CD98HC eliminates its transforming activity. Int J Cancer 2000; 87:311–316.
14. Nakamura E, Sato M, Yang H, Miyagawa F, Harasaki M, Tomita K, Matsuoka S, Noma A, Iwai K, Minato N. 4F2 (CD98) heavy chain is associated covalently with an amino acid transporter and controls intracellular trafficking and membrane topology of 4F2 heterodimer. J Biol Chem 1999;274:3009–3016.
15. Yanagida O, Kanai Y, Chairoungdua A, Kim DK, Segawa H, Nii T, Cha SH, Matsuo H, Fukushima J, Fukasawa Y, Tani Y, Taketani Y, et al. Human L-type amino acid transporter 1 (LAT1): characterization of function and expression in tumor cell lines. Biochim Biophys Acta 2001;1514:291–302.

16. Campbell WA, Sah DE, Medina MM, Albina JE, Coleman WB, Thompson NL. TA1/LAT-1/CD98 light chain and system L activity, but not 4F2/CD98 heavy chain, respond to arginine availability in rat hepatic cells. Loss of response in tumor cells. J Biol Chem 2000; 275:5347–54.
17. Samnick S, Bader JB, Hellwig D, Moringlane JR, Alexander C, Romeike BF, Feiden W, Kirsch CM. Clinical value of iodine-123-α-methyl-L-tyrosine single-photon emission tomography in the differential diagnosis of recurrent brain tumor in patients pretreated for glioma at follow-up. J Clin Oncol 2002;20:396–404.
18. Kuwert T, Probst-Cousin S, Woesler B, Morgenroth C, Lerch H, Matheja P, Palkovic S, Schafers M, Wassmann H, Gullotta F, Schober O. Iodine-123–methyltyrosine in gliomas: correlation with cellular density and proliferative activity. J Nucl Med 1997;38:1551–5.
19. Kaschten B, Stevenaert A, Sadzot B, Deprez M, Degueldre C, Del Fiore G, Luxen A, Reznik M. Preoperative evaluation of 54 gliomas by PET with fluorine-18-fluorodeoxyglucose and/or carbon-11-methionine. J Nucl Med 1998;39:778–85.
20. Langen KJ, Bonnie R, Muhlensiepen H, Jansen P, Broer S, Holschbach M, Coenen HH. 3-[123I]iodo-α-methyl-L-tyrosine transport and 4F2 antigen expression in human glioma cells. Nucl Med Biol 2001;28:5–11.
21. Shikano N, Kanai Y, Kawai K, Ishikawa N, Endou H. Characterization of 3-[125I]iodo-α-methyl-L-tyrosine transport via human L-type amino acid transporter 1. Nucl Med Biol 2003;30:31–7.
22. Langen KJ, Roosen N, Coenen HH, Kuikka JT, Kuwert T, Herzog H, Stocklin G, Feinendegen LE. Brain and brain tumor uptake of L-3-[123I]iodo–methyl tyrosine: competition with natural L-amino acids. J Nucl Med 1991;32:1225–8.
23. Storey BT, Fugere C, Lesieur-Brooks A, Vaslet C, Thompson NL. Adenoviral modulation of the tumor-associated system L amino acid transporter, LAT1, alters amino acid transport, cell growth and 4F2/CD98 expression with cell-type specific effects in cultured hepatic cells. Int J Cancer 2005;117:387–97.

J Pharmacol Sci 103, 48 – 55 (2007)

Journal of Pharmacological Sciences

Full Paper

Role of Mouse Organic Anion Transporter 3 (mOat3) as a Basolateral Prostaglandin E_2 Transport Pathway

Sirinun Nilwarangkoon[1], Naohiko Anzai[1], Katsuko Shiraya[1], Erkang Yu[1], Rafiqul Islam[1], Seok Ho Cha[1], Maristela Lika Onozato[2], Daisaku Miura[1], Promsuk Jutabha[1], Akihiro Tojo[2], Yoshikatsu Kanai[1], and Hitoshi Endou[1,*]

[1]*Department of Pharmacology and Toxicology, Kyorin University School of Medicine, 6-20-2 Shinkawa, Mitaka, Tokyo 181-8611, Japan*
[2]*Department of Nephrology and Endocrinology, University of Tokyo, 7-3-1, Hongo, Bunkyo-ku, Tokyo 113-8655, Japan*

Received July 24, 2006; Accepted November 14, 2006

Abstract. Renal organic anion transporters play an important role in the handling of a number of endogenous and exogenous anionic substances in the kidney. In this study, we investigated prostaglandin E_2 (PGE_2) transport properties and intrarenal localization of mouse organic anion transporter 3 (mOat3). When expressed in *Xenopus* oocytes, mOat3 mediated the time- and concentration-dependent transport of PGE_2 (K_m: 1.48 μM). PGE_2 transport mediated by mOat3 was *trans*-stimulated by intracellular glutarate injected into the oocytes. PGE_2 efflux via mOat3 was also *trans*-stimulated by extracellular glutarate. Thus, mOat3 was shown to mediate the bidirectional transport of PGE_2, partly coupled to the dicarboxylate exchange mechanism. Immunohistochemical study revealed that mOat3 protein was localized at the basolateral membrane of renal proximal and distal tubules. Furthermore, diffuse expression of mOat3, including expression in the basolateral membrane in macula densa (MD) cells, was observed. These results indicate that mOat3 plays an important role as a basolateral transport pathway of PGE_2 in the distal nephron including MD cells that may constitute one of the indispensable steps for renin release and regulation of the tubuloglomerular feedback mechanism.

Keywords: organic anion transporter, OAT, prostaglandin E_2, glutarate, macula densa

Introduction

Prostanoids, which include prostaglandins (PGs) and thromboxanes (TXs), are cyclooxygenase (COX)-dependent metabolites of arachidonic acids and play various physiological and pathophysiological roles (1, 2). Among them, PGE_2 is the major prostanoid in the kidney and is synthesized at high rates along the nephron, particularly in the collecting duct (3). PGE_2 plays an important role in the tubular reabsorption of salt and water as well as in the control of renal vascular resistance and the maintenance of glomerular hemodynamics. In addition, PGE_2 stimulates the release of renin from the juxtaglomerular apparatus (JGA). Recently, it has been reported that intact macula densa (MD) cells synthesize and release PGE_2 when luminal salt content is reduced, and it has been suggested that this response is involved in the control of renin release and renal vascular resistance during salt deprivation (4). In these functions, PGE_2 mediates autocrine and paracrine signaling over short distances through the activation of its four receptor subtypes (EP_1, EP_2, EP_3, and EP_4) (3). Thus, to maintain the extracellular concentration of PGE_2, the termination of PGE_2 signaling requires rapid re-uptake of released PGE_2 followed by cytoplasmic oxidation (5). Since PGE_2 possesses anionic moieties at physiological pH and diffuses poorly through the lipid bilayer, it is thought that PGE_2 transport across the plasma membrane is a carrier-mediated transport process (5). However, little is known about the molecular mechanism of the release of PGE_2 in distal nephron including MD cells.

To date, several PG carriers have been characterized (5). Prostaglandin transporter PGT (Slc21a2, oatp2A1)

*Corresponding author. endouh@kyorin-u.ac.jp
Published online in J-STAGE: January 13, 2007
doi: 10.1254/jphs.FP0060816

is broadly expressed in COX-positive cells and is coordinately regulated with COX. By analogy with neurotransmitter release and re-uptake, PGT may regulate pericellular PG levels via re-uptake (6). Immunocytochemical study has revealed that PGT in rat kidneys was expressed in glomerular endothelial and mesangial cells, arteriolar endothelial and muscularis cells, principal cells of the collecting duct, medullary interstitial cells, and the medullary vasa rectae endothelia (7). In the collecting duct, PGT is expressed in subapical vesicles. These results indicate that PGT is unlikely to be involved in the basolateral transport of PGE_2 in distal nephron including MD cells. Certain PGs are actively extruded from cells by multidrug resistance-associated proteins (MRPs) (5); these may play a role in metabolic clearance of PGs. However, the expression of MRPs in MD cells is still unclear.

Organic anion transporter (OAT) family members are other PG transporters (8). OATs play important roles in the elimination of a variety of endogenous substances, xenobiotics and their metabolites, many of which are potentially toxic to the body (9 – 14). Recently, cDNAs encoding OAT family members, including OAT1, OAT2, OAT3, OAT4, URAT1 (urate transporter 1), and Oat5, have been successively cloned (9). Among these clones, OAT1(human)/Oat1(rodents) and OAT3/Oat3 were shown to be localized to the basolateral side of the proximal tubule, whereas OAT4, URAT1, and Oat5 were shown to be localized to the apical side of the proximal tubule. In contrast, the exact localization of OAT2 protein in the kidney is still controversial: Rat Oat2 was formerly identified at the apical membrane of the thick ascending limb of Henle and cortical collecting ducts (15), but recently it has been shown to be localized at the apical side of proximal straight tubules (S_3 segment) (16), whereas human OAT2 was found to be localized to the basolateral membrane of the proximal tubule (17).

Among the OATs, OAT3 protein expression was detected in nearly all of the nephron segments in the rat kidney (15). Thus, OAT3 is likely to be a transporter responsible for the basolateral transport of PGE_2 in distal nephron including MD cells. Although Oat3 knockout mice have been generated several years ago (18), information on the functional properties of mouse Oat3 (mOat3) is limited (19 – 21). In this study, we examined PGE_2 transport properties and intrarenal localization of mOat3.

Materials and Methods

Materials

The materials used in this study were purchased from the following sources: [^{14}C]*p*-aminohippurate (PAH) (1.90 GBq/mmol) was from Moravek Biochemicals (Brea, CA, USA); [^{3}H]estrone-3-sulfate (E_1S) (2.0 TBq /mmol), [^{14}C]glutarate (2.035 GBq/mmol), and [^{3}H]PGE_2 (7.429 TBq/mmol) were from PerkinElmer Life Science Products (Boston, MA, USA); and glutarate was from Wako (Osaka). All other chemicals and reagents used were of analytical grade and obtained from commercial sources.

Animals

Six-week-old male ICR mice were purchased from Saitama Experimental Animal Co., Ltd. (Saitama) and kept under routine laboratory conditions with free access to standard laboratory chow and water.

Isolation of mOat3

A nondirectional cDNA library for screening was prepared from mouse kidney poly(A)$^-$ RNA using a Superscript Choice System (Invitrogen, Carlsbad, CA, USA) and was ligated into the phage vector ZipLox EcoRI arms (Invitrogen). The library was screened by homology using full-length rOat3 cDNA labeled with [^{32}P]dCTP by random priming (T7Quick Prime Kit; Amersham Pharmacia Biotech, Uppsala, Sweden) as a probe as described previously (22). cDNA inserts in positive ZipLox phages were recovered in the plasmid pZL1 vector by in vitro excision and completely sequenced with specially synthesized oligonucleotide primers by the dye terminator method using an ABI 3100 Genetic Analyzer (Applied Biosystems, Foster City, CA, USA).

cRNA synthesis and uptake experiments using Xenopus laevis oocytes

cRNA synthesis and uptake experiments were performed as described previously (23). The capped cRNA of mOat3 was synthesized in vitro by T7 RNA polymerase from a plasmid linearlized with Xba I. Defolliculated oocytes were injected with 10 ng of the capped mOat3 cRNA or water (control) and incubated in Barth's solution (88 mM NaCl, 1 mM KCl, 0.33 mM $Ca(NO_3)_2$, 0.4 mM $CaCl_2$, 0.8 mM $MgSO_4$, 2.4 mM $NaHCO_3$, and 10 mM HEPES) containing 50 μg/ml gentamicin at 18°C. After 2 to 3 days of incubation, uptake experiments of radiolabeled substrates, as indicated in each experiment, were performed at room temperature in ND96 solution (96 mM NaCl, 2 mM KCl, 1.8 mM $CaCl_2$, 1 mM $MgCl_2$, and 5 mM HEPES, pH 7.4). Each experiment was repeated more than two times to confirm the results. Representative results are shown in the figures.

Kinetic parameter for the uptake of PGE_2 via mOat3

was estimated from the following equation: $v = (V_{max} \times S) / (K_m + S)$, where v is the rate of substrate uptake (pmol/h·oocyte), S is the substrate concentration in the medium (μM), K_m is the Michaelis-Menten constant (μM), and V_{max} is the maximum uptake rate (pmol/h·oocyte). These kinetic parameters were determined with the Eadie-Hofstee equation.

To examine the *trans*-stimulatory effects of both the uptake and efflux of radiolabeled substrates, cold glutarate (50 mM) (Fig. 3) or 50 nl of [^{3}H]PGE_2 (0.6 μM) (Fig. 4) was injected into oocytes expressing mOat3 with a fine-tipped glass micropipette as described previously (24). Then individual oocytes were washed twice with ice-cold ND96 solution, placed on ice for 5 min, then incubated with ND96 at room temperature for 1 h, and finally transferred into a medium with or without radiolabeled E_1S (Fig. 3A) or PGE_2 (Fig. 3B) or with cold glutarate (10 mM) (Fig. 4) and incubated at room temperature for 1 h. [^{3}H]PGE_2 before and after taken up by the oocytes was little degraded as Chan et al. reported previously (25). Radioactivity in both the medium and oocytes was determined after a 1-h incubation.

For the uptake and efflux measurements in the present study, 8 – 10 oocytes were used for each data point. The values are expressed as means ± S.E.M. Each experiment was repeated at least twice to confirm the results. Results from representative experiments are shown in the figures.

Immunohistochemical analysis

For immunohistochemical analysis, rabbits were immunized with a keyhole limpet hemocyanin-conjugated synthesized peptide, CKASQTIPLKTGDPS, corresponding to cysteine and the 14 amino acids of the COOH terminus of mOat3. Two-micrometer wax sections of nephrectomized mouse kidney were processed for light microscopic immunohistochemical analysis using the streptavidin-biotin-horseradish peroxidase complex technique (LSAB kit; DAKO, Carpinteria, CA, USA). Sections were dewaxed, rehydrated, and incubated with 3% H_2O_2 for 10 min to eliminate endogenous peroxidase activity. After rinsing in 0.05 M Tris-buffered saline containing 0.1% Tween-20, sections were treated with 10 μg/ml of primary rabbit polyclonal antibody (at 4°C overnight). Thereafter, the sections were incubated with the secondary antibody, biotinylated goat polyclonal antibody against rabbit immunoglobulin (DAKO), diluted 1:400 for 30 min with horseradish peroxidase-labeled streptavidin. This step was followed by incubation with diaminobenzidine and hydrogen peroxide. The sections were counterstained with hematoxylin and examined by light microscopy. For a preabsorption experiment, the mOat3 peptide (200 μg/ml) was added to the mOat3-specific antibody solution and incubated overnight at 4°C. Using this preabsorbed antibody, immunohistochemistry was performed as described above.

Statistical analysis

Data are expressed as means ± S.E.M. Statistical differences were determined using Student's *t*-test. The reproducibility of the results in the present study was confirmed using two or three separate experiments. Results from representative experiments are shown in the figures.

Results

mOat3 cDNA was isolated from the kidney. As shown in Fig. 1, mOat3 mediated the transport of [^{14}C]PAH, [^{3}H]E_1S, [^{3}H]glutarate, and [^{3}H]PGE_2. These results indicate that our mOat3 clone is functional and its transport activity is compatible with that reported previously (18 – 20).

The uptake by mOat3 cRNA-injected oocytes increased linearly for about 180 min (Fig. 2A). Accord-

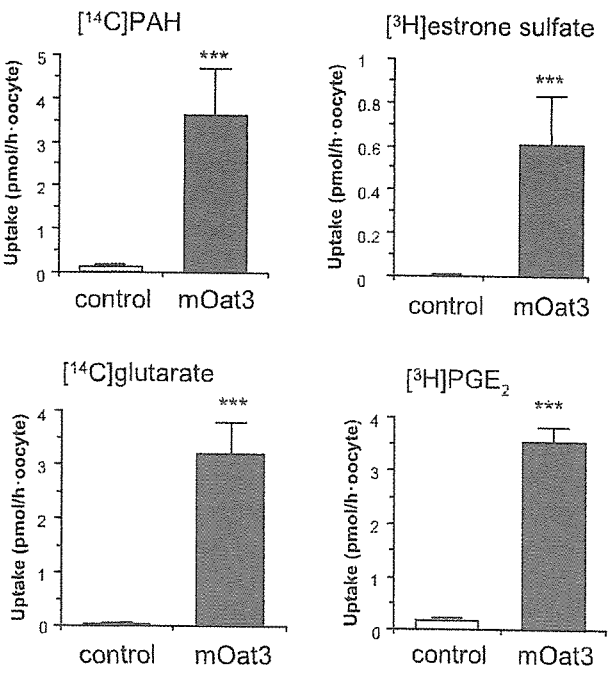

Fig. 1. Functional expression of mOat3 in *Xenopus* oocytes. mOat3 mediated the transport of several organic anions. The uptakes of radiolabeled [^{14}C]*p*-aminohippurate (PAH) (12 μM), [^{3}H]estrone sulfate (55 nM), [^{14}C]glutarate (5.5 μM), and [^{3}H]prostaglandin E_2 (PGE_2) (5 nM) by water-injected control oocytes and by mOat3-expressing oocytes were determined over a period of 1 h (mean ± S.E.M., n = 8 – 10). ***P<0.001 versus control.

ingly, analysis was performed at 60 min in the following experiments. The concentration dependence of the uptake of [^{3}H]PGE_2 via mOat3 is shown in Fig. 2B. The mOat3-mediated [^{3}H]PGE_2 uptake showed saturable kinetics and could be modeled by the Michaelis-Menten equation. Eadie-Hofstee plot analyses yielded a K_m value of 1.48 μM for PGE_2.

It is well established that OAT1 is a classical PAH /dicarboxylate exchanger (9). In addition, Sweet et al. and Bakhiya et al. reported that rat and human Oat3 /OAT3 functions as an organic anion/dicarboxylate exchanger (26, 27). Given the high sequence identity between rat Oat3 and mOat3, we assumed that their functions are very similar. However, a recent study by Ohtsuki et al. failed to demonstrate the E_1S/dicarboxylate exchange mechanism in mOat3 (19). Therefore, we next examined whether mOat3 is also organic anion /dicarboxylates exchanger or not. The uptake of [^{3}H]E_1S via mOat3 was *trans*-stimulated by the injection of cold glutarate into the oocytes (Fig. 3A). In addition, mOat3 mediated PGE_2/dicarboxylate exchange (Fig. 3B). We conclude that mOat3, as well as rat and human Oat3/OAT3, functions as an organic anion/dicarboxylate exchanger.

Then we examined the efflux of [^{3}H]PGE_2 from oocytes expressing mOat3. mOat3 exhibited significant efflux for [^{3}H]PGE_2, compared with water-injected

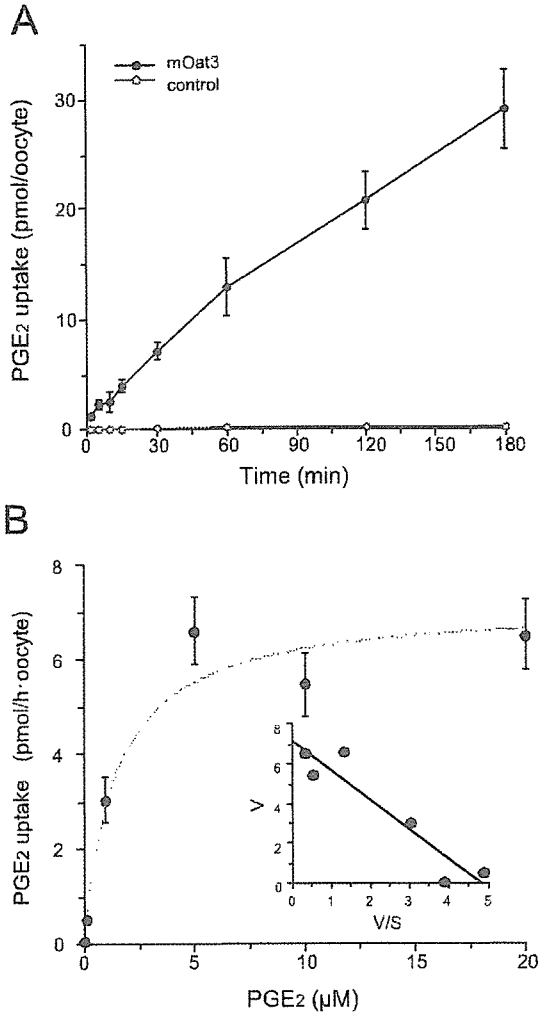

Fig. 2. Transport properties of PGE_2 via mOat3. A: Time-dependent uptake of [^{3}H]PGE_2 via mOat3. The uptake of 5 nM [^{3}H]PGE_2 was measured for 3 h in control oocytes and oocytes expressing mOat3 (mean ± S.E.M., n = 8 – 10). B: Concentration-dependence of mOat3-mediated uptake of PGE_2. The uptake rate of PGE_2 by control or mOat3-expressing oocytes for 1 h was measured at various concentrations (mean ± S.E.M., n = 8 – 10). Inset: Eadie-Hofstee plot. V, velocity; V/S, velocity per concentration of PGE_2.

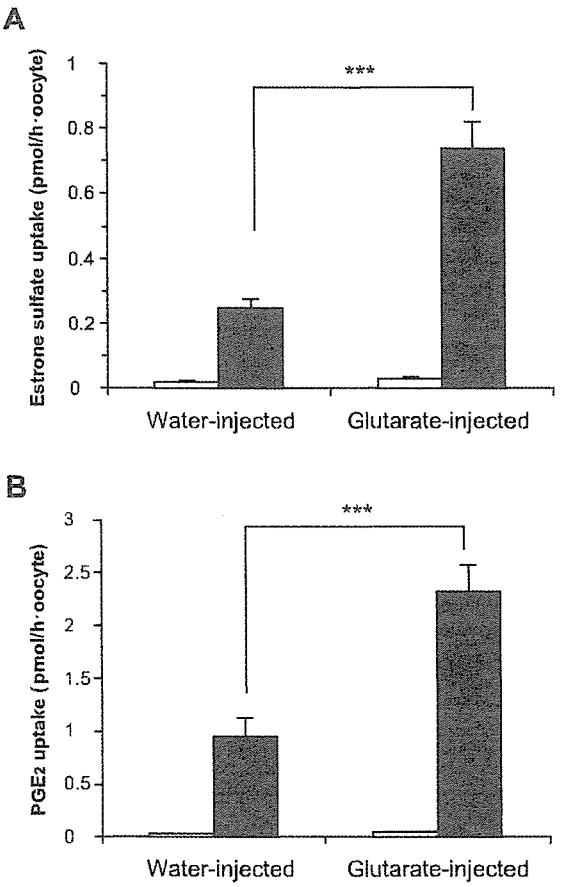

Fig. 3. Effects of glutarate on mOat3-mediated transport. *Trans*-stimulatory effect of glutarate on the uptake of [^{3}H]estrone sulfate (ES) (A) or [^{3}H]PGE_2 (B) via mOat3. Control (open column) and mOat3-expressing oocytes (closed column) were injected with 50 mM unlabeled glutarate (right columns) or water (left columns) and incubated for 5 min on ice. Then the oocytes were incubated with [^{3}H]ES (100 nM) or [^{3}H]PGE_2 (5 nM) and the amount of [^{3}H]ES or [^{3}H]PGE_2 accumulated for 1 h was determined (mean ± S.E.M., n = 8 – 10). ***P<0.001.

control oocytes (Fig. 4, left two columns). In addition, as would be expected for an exchanger, [^{3}H]PGE_2 efflux via mOat3 was significantly *trans*-stimulated by unlabeled glutarate in the medium (10 mM) (Fig. 4, right two columns).

Among the OAT isoforms, OAT3 as well as OAT1 are known to be polyspecific organic anion transporters that are responsible for the basolateral uptake of various organic anions (9 – 14). Although functional analysis of an Oat3 knockout mouse model strongly suggested that murine Oat3 was present in the basolateral membrane of renal proximal tubular cells (18), its exact localization in the kidney has not been demonstrated yet. Therefore, to clarify the intrarenal localization, we raised an antibody against the mOat3 C-terminal region and performed immunohistochemical analysis.

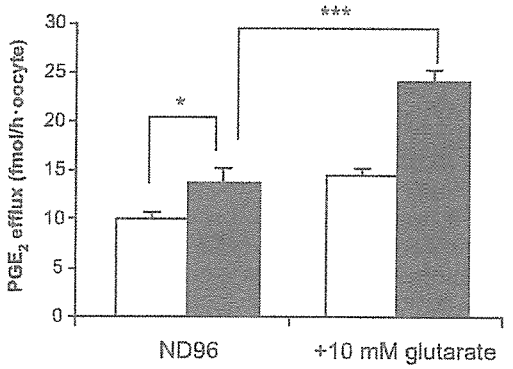

Fig. 4. mOat3-mediated butyrate efflux. *Trans*-stimulatory effect of glutarate on the efflux of [^{3}H]PGE_2 via mOat3. Control (open column) and mOat3-expressing (closed column) oocytes were injected with [^{3}H]PGE_2. After washing, the oocytes were incubated with 10 or 0 mM unlabeled glutarate. The amount of [^{3}H]PGE_2 effluxed for 1 h was determined. *P<0.05, ***P<0.001.

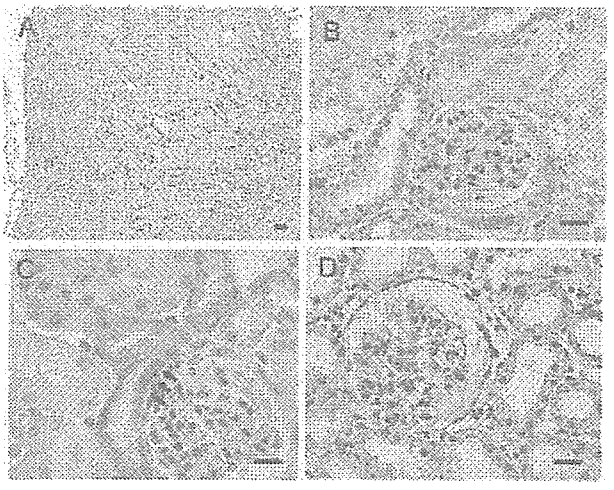

Fig. 5. Immunohistochemical analysis of Oat3 in mouse kidney. Two-micrometer sections were incubated with a polyclonal antibody against mOat3. Basolateral membrane of proximal tubules and that of distal tubules and collecting ducts were stained (proximal < distal), and no staining was observed in the glomeruli. Immunoreactivity in macula densa was also observed (arrows) at the basolateral side as well as the cytoplasm. (400×). Scale bars = 150 μm for A, 20 μm for B to D.

As shown in Fig. 5A, broad immunoreactivities of mOat3 were observed throughout the cortex under low magnification. There was no staining in the glomerulus. Under high magnification, mOat3 was found to be localized not only at the basolateral membrane of the proximal tubules but also at the same side of the distal tubules and of the collecting ducts (Fig. 5B). Interestingly, the intensities of mOat3 immunoreactivity seem stronger in the distal tubules and collecting ducts than in the proximal tubules. In addition, mOat3 immunoreactivity was detected in MD cells (Fig. 5C). By preincubation of the antibody with mOat3 peptide, the immunoreactivity disappeared (Fig. 5D). The specificity of the antibody for mOat3 was verified by these results.

Discussion

In this study, we analyzed mOat3-mediated PGE_2 transport properties and the intrarenal localization of mOat3 to determine whether mOat3 contributes to the basolateral transport of PGE_2 in distal nephron including MD cells.

PGE_2 is a major prostanoid derived from COX metabolism and modulates salt and water homeostasis in the kidney. In the renal cortex, COX-1 expression predominates in the collecting duct, vascular tissue, and glomerular mesangial cells, while COX-2 is expressed and presumably mediates PG production in the MD and surrounding cortical thick ascending limb (cTAL) cells (28 – 31). MD cells are in direct contact with the vascular pole of the same glomerulus from which the filtrate originates. They sense changes in tubular NaCl concentration and send signals to control preglomerular vascular resistance and glomerular filtration rate in a process named tubuloglomerular feedback (TGF). MD cells also control the renin release from juxtaglomerular granular cells (28 – 30). COX-2-derived PGs may participate in MD-mediated control of juxtaglomerular function, particularly in high renin states such as low salt intake, loop diuretic treatment, and renovascular hypertension (29, 31). PGE_2 produced by MD cells has been suggested to be the mediator of renin release induced by low luminal NaCl concentration (30 – 36). In addition, PGE_2, as a potent vasodilator, may also modulate preglomerular vascular resistance (3, 37) and TGF (38). Recently, it has been reported that PGE_2 release from MD cells is important in the control of renin release and

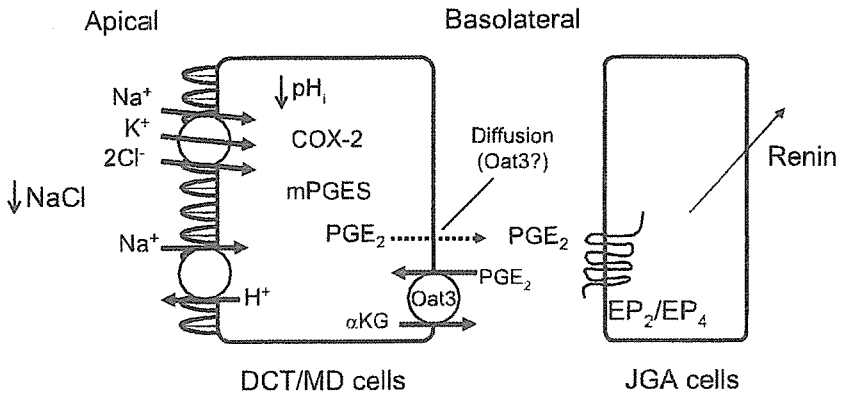

Fig. 6. Model of macula densa (MD) signaling. A marked decrease in tubular NaCl concentration, particularly under low salt diet, causes activation of the PG-synthesizing machinery, including COX-2 and microsomal PGE_2 synthase (mPGES) and PGE_2 release across the basolateral membrane via diffusion (or by Oat3). Oat3 is likely to be a transporter responsible for the rapid re-uptake of released PGE_2 using the outwardly directed gradient of dicarboxylates such as α-ketoglutarate (αKG).

renal vascular resistance during salt deprivation (4). However, little is known about the molecular mechanism of the transport of PGE_2 in distal nephron including MD cells.

The OAT family plays important roles in the elimination of a variety of endogenous substances, xenobiotics and their metabolites (9 – 14). We previously reported that human OATs (OAT1 to OAT4) mediate the transport of PGs (8). At present, there is little information on the functional properties of mouse Oat isoforms, particularly mOat3 (19 – 21), although Oat3 knockout mice have been generated several years ago (18). Among the OATs, OAT3 is likely to be a transporter responsible for the basolateral transport of PGE_2 in distal nephron including MD cells based on its broad localization in the rat kidney (15). In this regard, the current results support this possibility. mOat3 mediates both the uptake and the efflux of PGE_2 as shown in Figs. 2 – 4. Furthermore, mOat3 functions as an exchanger for both directions (Figs. 3 and 4). As shown in Fig. 5, mOat3 is localized at the basolateral membrane of proximal tubules, distal tubules including MD cells, and collecting ducts. These characteristics are compatible with the PGE_2 transport pathway in MD cells (Fig. 6).

As shown in Figs. 3 and 4, glutarate, a non-metabolized dicarboxylate, *trans*-stimulated mOat3-mediated PGE_2 transport in both directions. Taking the existence of the outwardly directed dicarboxylate gradient in tubular cells into account, endogenous dicarboxylates such as α-ketoglutarate (αKG) seem to contribute to the uptake of PGE_2 into cells. This supports the idea that Oat3 at the basolateral membrane of distal nephron functions as a re-uptake pathway of released PGE_2. As Pritchard mentioned (39), αKG is the most abundant within the proximal tubular cell. However, to date, there is no information concerning its concentration in distal nephron. Furthermore, energy-utilizing processes are different from segment to segment, based on the observation of ATP production in microdissected nephron segments shown by Uchida and Endou (40). Therefore, we could not exclude the possibility that Oat3 functions as an efflux pathway for PGE_2. As αKG is unlikely to be the endogenous counterion for PGE_2 efflux in MD cells, it seems necessary to identify such an endogenous counterion(s) for PGE_2 efflux in MD cells to further consider the role of PGE_2 as a signal, although the efflux of PGE_2 occurs without the counterion (Fig. 4).

Recently, Soodvilai et al. reported that the exposure of PGE_2 enhanced the OAT3-mediated estrone sulfate transport in isolated rabbit renal proximal tubules (41). Although no PGE_2-receptor isoform was detected in proximal tubules and distal tubules in renal cortex (3), this phenomenon seems compatible for the role of re-uptake of PGE_2 to maintain its extracellular concentration.

The K_m value for PGE_2 (1.48 μM) is different in humans and mice (more than 4-fold difference, ref. 8). The reason for this may be due to the interspecies difference in the interactions of OAT3/Oat3 with this substance or the difference in the expression system, that is, mammalian expression system for hOAT3 (8) versus *Xenopus* oocytes expression system for mOat3 (this study).

The generation of gene knockout animals could provide new information on the contribution of individual transporters in intact organs. Knockout mice for Oat3 have been generated several years ago (18). This model revealed the loss of organic anion transport and indicated the importance of drug uptake of Oat3 in the kidney and choroids plexus (42), although no morphological changes were found. Considering the novel role of mOat3 as a basolateral transport pathway of PGE_2 in MD cells, it would be interesting to observe changes in phenotype in mice under high renin states such as salt deficiency, administration of angiotensin-converting enzyme inhibitors or angiotensin receptor blockers, diuretic administration, or experimental renovascular

hypertension.

Since the molecular cloning of OAT1, first isoform of the OAT family, OATs were recognized mainly as an influx pathway of numerous endogenous and exogenous organic anions (12 – 14). However, recent studies by Aisf et al. unveiled the novel role of OAT3 as an efflux pathway of cortisol in endocrine tissues such as adrenocortical cells (43, 44). Therefore, the maintenance of homeostasis through the efflux of some endogenous substances such as PGs and steroid hormones would be another important role of the OAT family (9).

In conclusion, the current results indicate that mOat3 may play an important role in the basolateral efflux pathway of PGE_2 in the renal tubules including MD cells that may constitute one of the indispensable steps for renin release and the regulation of the TGF mechanism.

Acknowledgments

This work was supported in part by grants from the Ministry of Education, Culture, Sports, Science, and Technology of Japan; the Japan Society for the Promotion of Science; Research on Health Sciences focusing on Drug Innovation from the Japan Health Sciences Foundation; Mutual Aid Corporation for Private Schools of Japan; the Salt Science Research Foundation (No. 0524); the Japan Foundation of Applied Enzymology; Astellas Foundation for Research on Metabolic Disorders; Gout Research Foundation of Japan; The Ichiro Kanehara Foundation; The Shimabara Science Promotion Foundation; Kyorin University School of Medicine (Kyorin Medical Research Award 2006); and Health and Labor Sciences Research Grants for Research on Advanced Medical Technology: Toxicogenomics Project.

References

1 Narumiya S, Sugimoto Y, Ushikubi F. Prostanoid receptors: structures, properties, and functions. Physiol Rev. 1999;79: 1193–1226.
2 Ushikubi F, Sugimoto Y, Ichikawa A, Narumiya S. Roles of prostanoids revealed from studies using mice lacking specific prostanoid receptors. Jpn J Pharmacol. 2000;83:279–285.
3 Breyer MD, Breyer RM. G protein-coupled prostanoid receptors and the kidney. Annu Rev Physiol. 2001;63:579–605.
4 Peti-Peterdi J, Komlosi P, Fuson AL, Guan Y, Schneider A, Qi Z, et al. Luminal NaCl delivery regulates basolateral PGE_2 release from macula densa cells. J Clin Invest. 2003;112:76–82.
5 Schuster VL. Prostaglandin transport. Prostaglandins Other Lipid Mediat. 2002;68-69:633–647.
6 Bao Y, Pucci ML, Chan BS, Lu R, Ito S, Schuster VL. Prostaglandin transporter PGT is expressed in cell types that synthesize and release prostanoids. Am J Physiol Renal Physiol. 2002;282:F1103–F1110.
7 Kimura H, Takeda M, Narikawa S, Enomoto A, Ichida K, Endou H. Human organic anion transporters and human organic cation transporters mediate renal transport of prostaglandins. J Pharmacol Exp Ther. 2002;301:293–298.
8 Nomura T, Chang HY, Lu R, Hankin J, Murphy RC, Schuster VL. Prostaglandin signaling in the renal collecting duct: release, reuptake, and oxidation in the same cell. J Biol Chem. 2005;280:28424–28429.
9 Anzai N, Kanai Y, Endou H. Organic anion transporter family: current knowledge. J Pharmacol Sci. 2006;100:411–426.
10 Sekine T, Miyazaki H, Endou H. Molecular physiology of renal organic anion transporters. Am J Physiol Renal Physiol. 2006;290:F251–F261.
11 Anzai N, Jutabha P, Kanai Y, Endou H. Integrated physiology of proximal tubular organic anion transport. Curr Opin Nephrol Hypertens. 2005;14:472–479.
12 Wright SH, Dantzler WH. Molecular and cellular physiology of renal organic cation and anion transport. Physiol Rev. 2004;84:987–1049.
13 You G. The role of organic ion transporters in drug disposition: an update. Curr Drug Metab. 2004;5:55–62.
14 Burckhardt BC, Burckhardt G. Transport of organic anions across the basolateral membrane of proximal tubule cells. Rev Physiol Biochem Pharmacol. 2003;146:95–158.
15 Kojima R, Sekine T, Kawachi M, Cha SH, Suzuki Y, Endou H. Immunolocalization of multispecific organic anion transporters, OAT1, OAT2, and OAT3, in rat kidney. J Am Soc Nephrol. 2002;13:848–857.
16 Ljubojevic M, Balen D, Breljak D, Kusan M, Anzai N, Bahn A, et al. Renal expression of organic anion transporter OAT2 in rats and mice is regulated by sex hormones. Am J Physiol Renal Physiol. 2007;292:F361–F372.
17 Enomoto A, Takeda M, Shimoda M, Narikawa S, Kobayashi Y, Kobayashi Y, et al. Interaction of human organic anion transporters 2 and 4 with organic anion transport inhibitors. J Pharmacol Exp Ther. 2002;301:797–802.
18 Sweet DH, Miller DS, Pritchard JB, Fujiwara Y, Beier DR, Nigam SK. Impaired organic anion transport in kidney and choroid plexus of organic anion transporter 3 (Oat3 (*Slc22a8*)) knockout mice. J Biol Chem. 2002;277:26934–26943.
19 Ohtsuki S, Kikkawa T, Mori S, Hori S, Takanaga H, Otagiri M, et al. Mouse reduced in osteosclerosis transporter functions as an organic anion transporter 3 and is localized at abluminal membrane of blood-brain barrier. J Pharmacol Exp Ther. 2004;309:1273–1281.
20 Kobayashi Y, Ohshiro N, Tsuchiya A, Kohyama N, Ohbayashi M, Yamamoto T. Renal transport of organic compounds mediated by mouse organic anion transporter 3 (mOat3): further substrate specificity of mOat3. Drug Metab Dispos. 2004;32: 479–483.
21 Bahn A, Ljubojevic M, Lorenz H, Schultz C, Ghebremedhin E, Ugele B, et al. Murine renal organic anion transporters mOAT1 and mOAT3 facilitate the transport of neuroactive tryptophan metabolites. Am J Physiol Cell Physiol. 2005;289:C1075–C1084.
22 Sakata T, Anzai N, Shin HJ, Noshiro R, Hirata T, Yokoyama H, et al. Novel single nucleotide polymorphisms of organic cation transporter 1 (*SLC22A1*) affecting transport functions. Biochem Biophys Res Commun. 2004;313:789–793.
23 Anzai N, Jutabha P, Enomoto A, Yokoyama H, Nonoguchi H,

Hirata T, et al. Functional characterization of rat organic anion transporter 5 (*Slc22a19*) at the apical membrane of renal proximal tubules. J Pharmacol Exp Ther. 2005;315:534–544.
24 Jutabha P, Kanai Y, Hosoyamada M, Chairoungdua A, Kim do K, Iribe Y, et al. Identification of a novel voltage-driven organic anion transporter present at apical membrane of renal proximal tubule. J Biol Chem. 2003;278:27930–27938.
25 Chan BS, Satriano JA, Pucci M, Schuster VL. Mechanism of prostaglandin E2 transport across the plasma membrane of HeLa cells and Xenopus oocytes expressing the prostaglandin transporter "PGT". J Biol Chem. 1998;273:6689–6697.
26 Sweet DH, Chan LM, Walden R, Yang XP, Miller DS, Pritchard JB. Organic anion transporter 3 (*Slc22a8*) is a dicarboxylate exchanger indirectly coupled to the Na^+ gradient. Am J Physiol Renal Physiol. 2003;284:F763–F769.
27 Bakhiya N, Bahn A, Burckhardt G, Wolff NA. Human organic anion transporter 3 (hOAT3) can operate as an exchanger and mediate secretory urate flux. Cell Physiol Biochem. 2003; 13:249–256.
28 Smith WL, Bell TG. Immunohistochemical localization of the prostaglandin-forming cyclooxygenase in renal cortex. Am J Physiol. 1978;235:F451–F457.
29 Harris RC, McKanna JA, Akai Y, Jacobson HR, Dubois RN, Breyer MD. Cyclooxygenase-2 is associated with the macula densa of rat kidney and increases with salt restriction. J Clin Invest. 1994;94:2504–2510.
30 Schnermann J. Cyclooxygenase-2 and macula densa control of renin secretion. Nephrol Dial Transplant. 2001;16:1735–1738.
31 Harris RC, Wang JL, Cheng HF, Zhang MZ, McKanna JA. Prostaglandins in macula densa function. Kidney Int. 1998;67: S49–S52.
32 Schnermann J, Briggs J. Function of the juxtaglomerular apparatus: local control of glomerular hemodynamics. In: Seldin DW, Giebisch G, editors. The kidney. New York: Raven Press; 1985. p. 669–697.
33 Harris RC, Breyer MD. Physiological regulation of cyclooxygenase-2 in the kidney. Am J Physiol Renal Physiol. 2001;281:F1–F11.
34 Yang T, Endo Y, Huang YG, Smart A, Briggs JP, Schnermann J. Renin expression in COX-2-knockout mice on normal or low-salt diets. Am J Physiol Renal Physiol. 2000;279:F819–F825.
35 Castrop H, Schweda F, Schumacher K, Wolf K, Kurtz A. Role of renocortical cyclooxygenase-2 for renal vascular resistance and macula densa control of renin secretion. J Am Soc Nephrol 2001;12:867–874.
36 Traynor TR, Smart A, Briggs JP, Schnermann J. Inhibition of macula densa-stimulated renin secretion by pharmacological blockade of cyclooxygenase-2. Am J Physiol 1999;277:F706–F710.
37 Chaudhari A, Gupta S, Kirschenbaum MA. Biochemical evidence for PGI_2 and PGE_2 receptors in the rabbit renal preglomerular microvasculature. Biochim Biophys Acta. 1990;1053:156–161.
38 Schnermann J, Weber PC. Reversal of indomethacin-induced inhibition of tubuloglomerular feedback by prostaglandin infusion. Prostaglandins. 1982;24:351–361.
39 Pritchard JB. Intracellular alpha-ketoglutarate controls the efficacy of renal organic anion transport. J Pharmacol Exp Ther. 1995;274:1278–1284.
40 Uchida S, Endou H. Substrate specificity to maintain cellular ATP along the mouse nephron. Am J Physiol. 1988;255:F977–F983.
41 Soodvilai S, Chatsudthipong V, Evans KK, Wright SH, Dantzler WH. Acute regulation of OAT3-mediated estrone sulfate transport in isolated rabbit renal proximal tubules. Am J Physiol Renal Physiol. 2004;287:F1021–F1029.
42 Sykes D, Sweet DH, Lowes S, Nigam SK, Pritchard JB, Miller DS. Organic anion transport in choroid plexus from wild-type and organic anion transporter 3 (*Slc22a8*)-null mice. Am J Physiol Renal Physiol. 2004;286:F972–F978.
43 Asif AR, Steffgen J, Metten M, Grunewald RW, Muller GA, Bahn A, et al. Presence of organic anion transporters 3 (OAT3) and 4 (OAT4) in human adrenocortical cells. Pflugers Arch. 2005;450:88–95.
44 Asif AR, Ljubojevic M, Sabolic I, Shnitsar V, Metten M, Anzai N, et al. Regulation of steroid hormone biosynthesis enzymes and organic anion transporters by forskolin and DHEAS treatment in adrenocortical cells. Am J Physiol Endocrinol Metab. 2006; 291:E1351–E1359.

J Pharmacol Sci 100, 411 – 426 (2006)

Journal of Pharmacological Sciences

Review

Organic Anion Transporter Family: Current Knowledge

Naohiko Anzai[1], Yoshikatsu Kanai[1], and Hitoshi Endou[1,2,*]

[1]*Department of Pharmacology and Toxicology, Kyorin University School of Medicine, 6-20-2, Shinkawa, Mitaka-shi, Tokyo 181-8611, Japan*
[2]*Fuji Biomedix Co., Ltd., 6-25-10, Tsukiji, Chuo-ku, Tokyo 101-0045, Japan*

Received March 23, 2006

Abstract. Organic anion transporters (OATs) play an essential role in the elimination of numerous endogenous and exogenous organic anions from the body. The renal OATs contribute to the excretion of many drugs and their metabolites that are important in clinical medicine. Several families of multispecific organic anion and cation transporters, including OAT family transporters, have recently been identified by molecular cloning. The OAT family consists of six isoforms (OAT1 – 4, URAT1, and rodent Oat5) and they are all expressed in the kidney, while some are also expressed in the liver, brain, and placenta. The OAT family represents mainly the renal secretory and reabsorptive pathway for organic anions and is also involved in the distribution of organic anions in the body, drug-drug interactions, and toxicity of anionic substances such as nephrotoxic drugs and uremic toxins. In this review, current knowledge of and recent progress in the understanding of several aspects of OAT family members are discussed.

Keywords: organic anion, *p*-aminohippurate, organic anion transporter (OAT), kidney

*Corresponding author (affiliation #1). endouh@kyorin-u.ac.jp
Published online in J-STAGE
DOI: 10.1254/jphs.CRJ06006X

Invited article

1. Introduction

A variety of endogenous and exogenous substances that are harmful to the body can be classified into organic anions and cations. Their elimination is essential for the maintenance of homeostasis. Excretory organs such as the kidneys, liver, and intestine defend the body against potentially harmful effects of these compounds by biotransformation into less active metabolites and by the excretory transport process. In the kidney, drugs and environmental toxicants are eventually excreted into the urine, either in an unchanged form or as biotransformation products. This renal excretion is closely related to physiological events occurring in nephrons, i.e., filtration, secretion, and reabsorption. It was observed more than 70 years ago that phenolsulphophthalein, an anionic dye, was highly concentrated in renal convoluted tubules, suggesting a tubular secretion process (1). Transport systems responsible for renal tubular secretion of endogenous or exogenous substances have been

Table 1. Organic anion transporter (OAT) family

Gene name	Protein name	Tissue distribution	Predominant substrates
SLC22A6	OAT1	kidney	PAH, PGE_2, urate, NSAIDs, antiviral agents, MTX, OTA, β-lactam antibiotics, ACE inhibitors, uremic toxins
SLC22A7	OAT2	liver	PGE_2, $PGF_{2\alpha}$, tetracycline
SLC22A8	OAT3	kidney, brain	ES, cAMP, cGMP, $E_2 17\beta G$, DHEAS, PGE_2, $PGF_{2\alpha}$, OTA, MTX, cimetidine, tetracycline, uremic toxins
SLC22A11	OAT4	kidney, placenta	ES, DHEAS, PGE_2, $PGF_{2\alpha}$, tetracycline, MTX, OTA
SLC22A12	URAT1	kidney	urate
Slc22a19	Oat5	kidney	ES, DHEAS, OTA

PAH, *p*-aminohippurate; PG, prostaglandin; NSAIDs, nonsteroidal inflammatory drugs; MTX, methotrexate; OTA, ochratoxin A; ACE, angiotensin-converting enzyme; ES, estrone sulfate; $E_2 17\beta G$, estradiol 17β-D-glucuronide; DHEAS, dehydroepiandrosterone sulfate.

divided into organic anion and organic cation transport systems based on their preferential substrate selectivity (2). The process of secreting organic anions and cations through proximal tubular cells is achieved via unidirectional transcellular transport, involving the uptake of organic ions into the cells from the blood across the basolateral membrane followed by extrusion across the brush-border membrane into the proximal tubular fluid (3). During the last decade, several families of multispecific organic anion transporters, including organic anion transporter (OAT) family (Table 1), organic anion-transporting polypeptide (oatp) family, sodium-phosphate transporter (NPT) family, and peptide transporter (PEPT) family, has been identified by molecular cloning (Fig. 1). Additional findings also suggested ATP-dependent organic anion transporters such as multidrug resistance-associated protein (MRP) as efflux pumps (Fig. 1). This review focuses on the recent progress in the understanding of various aspects of the OAT family. A number of reviews (4 – 9) on organic anion transporters are available.

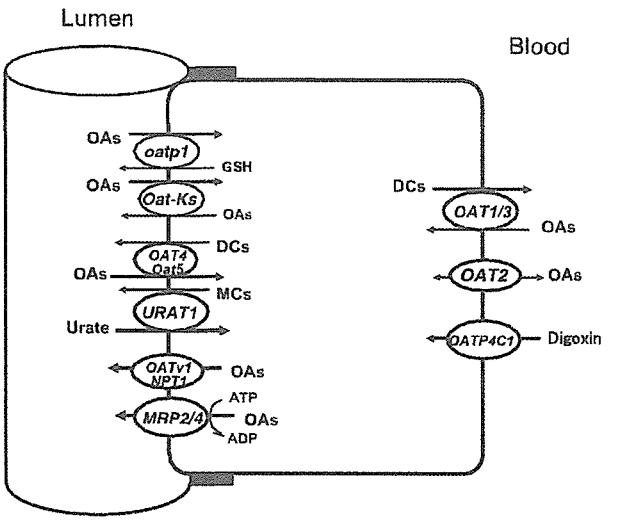

Fig. 1. Proposed model of organic anion transporters in renal proximal tubules. OAs: organic anions, DCs: dicarboxylates, MCs: monocarboxylates.

2. General characteristics of OATs

2.1. Organic anion transport systems

Substrates for the renal organic anion transport system include a number of chemically heterogeneous weak acids with a carbon backbone and a net negative charge at physiological pH (pK_a <7). Their structures may be aromatic or aliphatic. Historically, *p*-aminohippurate (PAH) has been used as a prototypical substrate for the renal organic anion transport system (2). PAH is a high-affinity substrate and is almost completely extracted by the renal organic anion transport system during a single pass through the kidney when its serum concentration is low. Thus, PAH clearance has been used to estimate renal plasma flow, and the renal organic anion transporter has been alternatively called PAH transporter. A prominent feature of the PAH transporter is that it interacts with and transports a variety of organic anions with unrelated chemical structures (2 – 4). Various endogenous organic anions, uremic substances, drugs, and environmental compounds have been assumed to be substrates of the PAH transporter. The multispecificity of the PAH transporter is suitable for elimination of a variety of endogenous metabolites and xenobiotics; and in renal physiology, the PAH transport system has been regarded as a representative of "tubular secretion". In 1997, the PAH transporter was isolated by several groups using expression cloning methods and designated OAT1 (organic anion transporter 1) (10 – 12). Subsequently, several organic anion-transporting proteins have been identified at both sides of the renal proximal tubules and our knowledge of

organic anion transporter systems has been increased (Fig. 1).

2.2. Functional characteristics of organic anion transport systems

In the kidney, the secretion of organic anions takes place in the proximal tubular epithelial cells via at least two steps. The first step is the transport of organic anions from the peritubular plasma across the basolateral membrane into proximal tubular cells. The transport of PAH across the basolateral membrane of proximal tubular cells against the electrochemical gradient occurs in exchange for intracellular dicarboxylates such as α-ketoglutarate (13). Two organic anion transporters, OAT1 (10 – 12) and OAT3 (14), have been proposed to be responsible for this step. The second step is the exit of organic anions across the apical membrane at the tubular epithelial cells into the urine. Although this process is energetically downhill for organic anions, it has been believed that this process is also mediated by specific transporters. The luminal efflux system for PAH has been investigated mostly using brush border membrane vesicles. In dogs and rats, anion exchange mechanisms have been demonstrated for the luminal efflux systems (15). They mediate probenecid-sensitive electroneutral exchange of anionic compounds, including both organic (e.g., PAH, urate, and lactate) and inorganic (e.g., Cl^-, HCO_3^-, OH^-) anions. A distinct efflux system involving voltage-driven transport was demonstrated in the pig and rabbit (15). PAH transport at the apical membrane in the OK kidney epithelial cell line was shown to be mediated by a voltage-driven transport system but not by an anion exchange system (16). In physiological conditions, a major component of the exit path of organic anions from renal proximal tubular cells has been proposed to be the facilitated diffusion along the electrochemical potential gradient (3, 17). Voltage-driven organic anion transport plays an important role in this step. However, the molecular nature and precise functional properties of these efflux systems were unknown for a long time.

2.3. Molecular identification of OATs

OAT1: Several research groups have cloned the first member of the OAT family, OAT1 (10 – 12). OAT1 mRNA is expressed predominantly in the kidneys and weakly in the brain. In the kidneys, OAT1 protein is localized at the basolateral membrane of proximal tubular cells. OAT1-mediated uptake of PAH is stimulated by an outwardly directed concentration gradient of dicarboxylates such as α-ketoglutarate, which is consistent with the previous notion that OAT1 is an organic anion-dicarboxylate exchanger (13). The substrate selectivity of OAT1 is markedly broad, and substrates include endogenous substances such as dicarboxylates, cyclic nucleotides, and prostaglandins and exogenous substances such as various anionic drugs and environmental compounds (15). The affinities of OAT1 for these compounds are similar to reported values for the basolateral PAH transporter (2), and the functional properties and localization of OAT1 are identical to those of the renal PAH transport system.

OAT2: OAT2 was isolated originally from the rat liver as a novel liver-specific transport protein with unknown function (18). Because of its structural similarities to OAT1, OAT2 was functionally characterized (19). OAT2 is expressed predominantly in the liver and weakly in the kidneys. Typical substrates of OAT2 are salicylate, acetylsalicylate, prostaglandin E_2 (PGE_2), dicarboxylates, and PAH. Transport of tetracycline by hOAT2 as well as other hOATs has been also reported by us (20). Recently, hOAT2 was proposed to be a sodium-independent multi-specific organic anion/dimethyldicarboxylate exchanger (21).

OAT3: OAT3 was isolated from the rat (14), and it seems to us structurally identical to Roct, which has been identified as a transporter-like protein that exhibits a reduced expression in osteosclerosis mice (22). OAT3 mRNA is expressed in the kidneys, liver, brain and eyes (14). In the kidneys, OAT3 is localized at the basolateral membrane of proximal tubular cells (23, 24). In the brain, OAT3 is localized at the brush border membrane of choroid plexus cells (25, 26) and in capillary endothelial cells (27). Like OAT1, OAT3 recognizes a broad spectrum of substrates, and it mediates the high-affinity transport of PAH, estrone sulfate, ochratoxin A, and various drugs, including the cationic drug cimetidine, in exchange for dicarboxylates inside cells (28, 29).

OAT4: OAT4 was cloned from human kidneys (30). OAT4 mRNA is expressed in the kidneys and is localized at the apical membrane of proximal tubular cells. In the placenta, OAT4 is expressed on the foetal side of syncytiotrophoblast cells (31). When expressed in *Xenopus* oocytes, OAT4 mediates the Na^--independent, high-affinity transport of estrone sulfate, dehydroepiandrosterone sulfate, ochratoxin A, and PGE_2 and $PGF_{2\alpha}$. We recently reported that OAT4 is not a facilitated transporter but an organic anion/dicarboxylate exchanger and that it mediates bidirectional organic anion transport (32). The results indicate that OAT4 is a renal apical organic anion/dicarboxylate exchanger and mainly serves as a tubular reabsorptive pathway for some organic anions, including sulfate conjugates, driven by an outwardly directed gradient of dicarboxylates such as α-ketoglutarate. However, it seems unlikely that two exchangers of the same type existing in both